Friction **11**(12): 2153–2180 (2023)
https://doi.org/10.1007/s40544-022-0702-x

ISSN 2223-7690
CN 10-1237/TH

REVIEW ARTICLE

Interfacial friction at action: Interactions, regulation, and applications

Zhiran YI[1,2,3], **Xiong WANG**[1], **Wanbo LI**[1], **Xuezhi QIN**[1], **Yang LI**[1], **Kaiqiang WANG**[1,4], **Yunting GUO**[1,5], **Xing LI**[1], **Wenming ZHANG**[3], **Zuankai WANG**[1,2,*]

[1] *Department of Mechanical Engineering, City University of Hong Kong, Hong Kong 999077, China*

[2] *Hong Kong Centre for Cerebro–caradiovasular Health Engineering (COCHE), Hong Kong 999077, China*

[3] *State Key Laboratory of Mechanical System and Vibration, School of Mechanical Engineering, Shanghai Jiao Tong University, Shanghai 200240, China*

[4] *State Key Laboratory of Tribology in Advanced Equipment, Tsinghua University, Beijing 100084, China*

[5] *Key Laboratory of Bionic Engineering, Ministry of Education, Jilin University, Changchun 130022, China*

Received: 03 May 2022 / Revised: 09 September 2022 / Accepted: 27 September 2022

Abstract: Friction is a fundamental force that impacts almost all interface-related applications. Over the past decade, there is a revival in our basic understanding and practical applications of the friction. In this review, we discuss the recent progress on solid–liquid interfacial friction from the perspective of interfaces. We first discuss the fundamentals and theoretical evolution of solid–liquid interfacial friction based on both bulk interactions and molecular interactions. Then, we summarize the interfacial friction regulation strategies manifested in both natural surfaces and artificial systems, focusing on how liquid, solid, gas, and hydrodynamic coupling actions mediate interfacial friction. Next, we discuss some practical applications that are inhibited or reinforced by interfacial friction. At last, we present the challenges to further understand and regulate interfacial friction.

Keywords: interfacial friction; solid–liquid interface; interfacial interaction; friction regulation

1 Introduction

Friction, as a fundamental force in tribology, penetrates almost every corner of our lives from solid–solid and solid–liquid to liquid–liquid interfaces. Friction at the solid–liquid interface impacts many significant applications [1, 2] including both bright and dark sides. The former lies in maximizing the interfacial friction for high-efficient interfacial energy transfer or mass transport, involving energy harvesting [3, 4], cooling [5], micro-/nano-fluidics [6, 7], wetting [8, 9], and water harvesting [10, 11]. On the contrary, the latter needs to minimize the interfacial friction as much as possible for low energy loss or high mechanical reliability, mainly involving biological lubrication [12, 13], anti-fouling [14, 15], drag reduction [16–18], liquid transfer [19, 20], and liquid operation [21, 22] (Fig. 1). Effectively implementing these applications recalls our fundamental understanding and regulation of interfacial friction behaviors.

Friction is not a new concept. The fundamental understanding of interfacial friction began with the distinction of motion resistance in sliding and rolling motions by Leonardo da Vinci 500 years ago [23–25]. Since then, investigating interfacial friction mainly focuses on macroscopic interaction that how the interfacial friction behaviors are affected by the applied load, contact area, and sliding velocity involved in macroscopic solid motions, which lay down the foundation of the classical dry friction laws [26–30]. Yet, the underlying interfacial friction behaviors at microscopic were invisible and mysterious owing

---

* Corresponding author: Zuankai WANG, E-mail: zk.wang@polyu.edu.hk

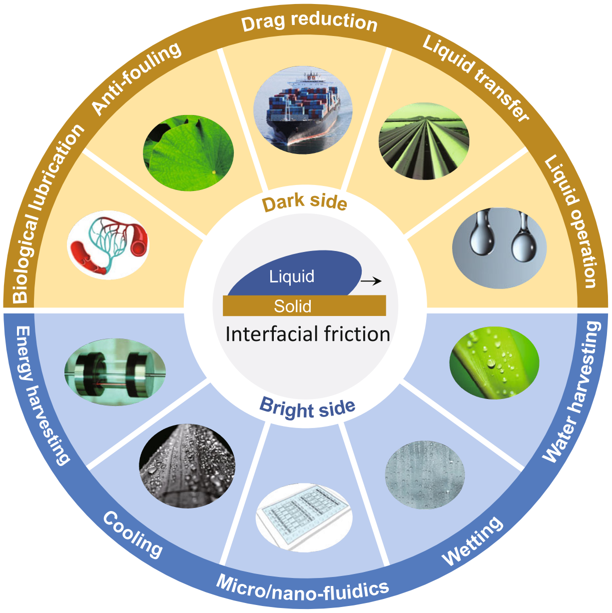

Fig. 1 Impact of interfacial friction on diverse fields.

to the complexity of friction behaviors imposed by multi-scale, multi-physic, and multi-phase combinative effects, which trigger more curiosity for the investigation of interfacial friction. The development in microscopic visualization, biomimetic surfaces, high-precision probing techniques, and molecular dynamics theory led to a revival in the microscopic interfacial friction behaviors, as reflected by the gradual clarification of the evolution of microscopic morphology, the migration of charge carriers, the origination of microscopic interfacial interaction, and the transformation of phase types. Particularly, many fantastic friction behaviors in the nature provide a lot of unique insights for our understanding. Recently, a new landscape involving macroscopic and microscopic interfacial friction, especially in solid–liquid interfaces, was revealing the interfacial friction behaviors of multi-scale combinative effect with the tremendous progress in interface science and techniques, such as quantum interaction [31], superhydrophobic surface [32], and high-dimensional biomimetic system [6, 33].

Currently, interfacial friction can be regulated by the control of the macroscopic and microscopic interfacial interactions, affected by internal medium characteristics and external stimuli. In macroscopic, the interfacial interaction mainly relies on the bulk structures of internal mediums and their dynamic behaviors and can be regarded as interfacial bulk interactions. In microscopic, the interfacial interaction is dominated by the interfacial molecular interactions, mainly affected by the material characteristics of interfacial mediums and external stimuli. Notably, without delicate control of the bulk and molecular interactions, the interfacial friction regulation will be limited to relatively poor durability of interfacial structures, mass loss, and additional energy consumption. However, a timely summary of solid–liquid interfacial friction interaction and regulation strategies is still lacking.

In this review, we discuss the latest progress in the development of interfacial friction from the perspectives of interfaces, especially solid–liquid interfaces. First, we review the fundamentals of interfacial friction including interfacial bulk interactions and interfacial molecular interactions. Then, we take a parallel treatment between natural surfaces and artificial systems to summarize the interfacial friction regulation strategies, mainly focusing on liquid, gas, solid, and hydrodynamic coupling-mediated solid–liquid interfaces (Fig. 2). We also highlight both sides of solid–liquid interfacial friction behaviors and discuss their representative applications. At last, we discuss challenges and future perspectives for the further development of solid–liquid interfacial friction.

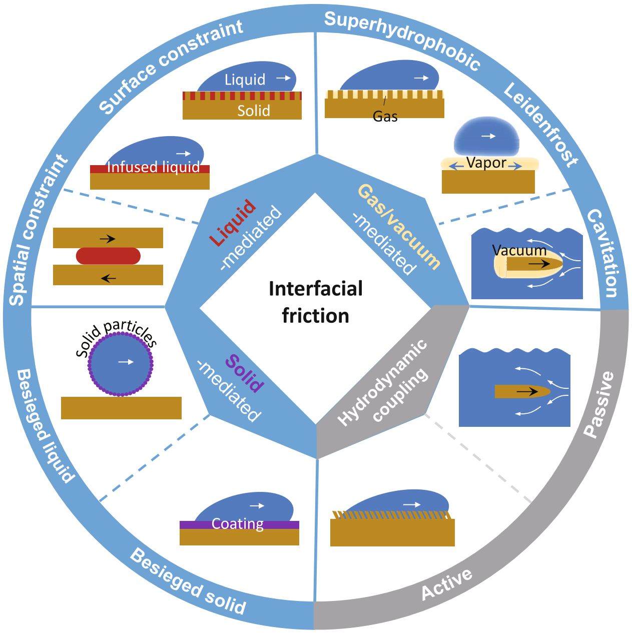

Fig. 2 Overview of interfacial friction regulation strategies from the perspective of interfaces, including phase (liquid, gas, and solid)-mediated and hydrodynamic coupling-mediated interfaces.

2 Fundamentals of interfacial friction

Interfacial friction is manifested as a resistance phenomenon [34–38], which is rooted in interfacial interactions triggered by interfacial dynamic behaviors and electromagnetic effects. Following such fundamental understanding, interfacial interactions are classified as interfacial bulk interactions and interfacial molecular interactions. Originating from these interfacial interactions, interfacial friction can be delivered as diverse types, which will be introduced in detail in Section 2.

2.1 Interfacial bulk interactions

Interfacial bulk interactions, defined as the interactions of inertia forces induced by interfacial dynamic behaviors, are closely associated with the dynamic characteristics and surface morphologies of the interfacial mediums (Fig. 3(a)). On the one hand, the dynamic characteristics, such as laminar flow or turbulent flow (Fig. 3(b)), provide the basic driving force for interfacial bulk interactions. On the other hand, the surface morphologies dominate the interfacial contact characteristics, which affect the transmission of the inertia force. Briefly, the interfacial bulk interactions could be considered as a manifestation of the dynamic behaviors regardless of macroscopic or microscopic interfaces.

Different bulk interactions based on dynamic behaviors can bring about diverse types of interfacial friction, such as sliding, stick–slip, rolling, or lubricated frictions (Fig. 3(c)). Among these frictions, the sliding and stick–slip frictions are classified by liquid flow characteristics. For example, sliding friction [39, 40] mainly describes the sliding motion resistance of the liquid on solid surfaces. If the interfacial interactions are nonuniform in the liquid sliding process, the liquid may perform a stick–slip motion behavior, in which the motion resistance is described as the stick–slip friction combined with dynamic and static characteristics [41–43]. Besides, the rolling and lubricated frictions mainly involve different motion

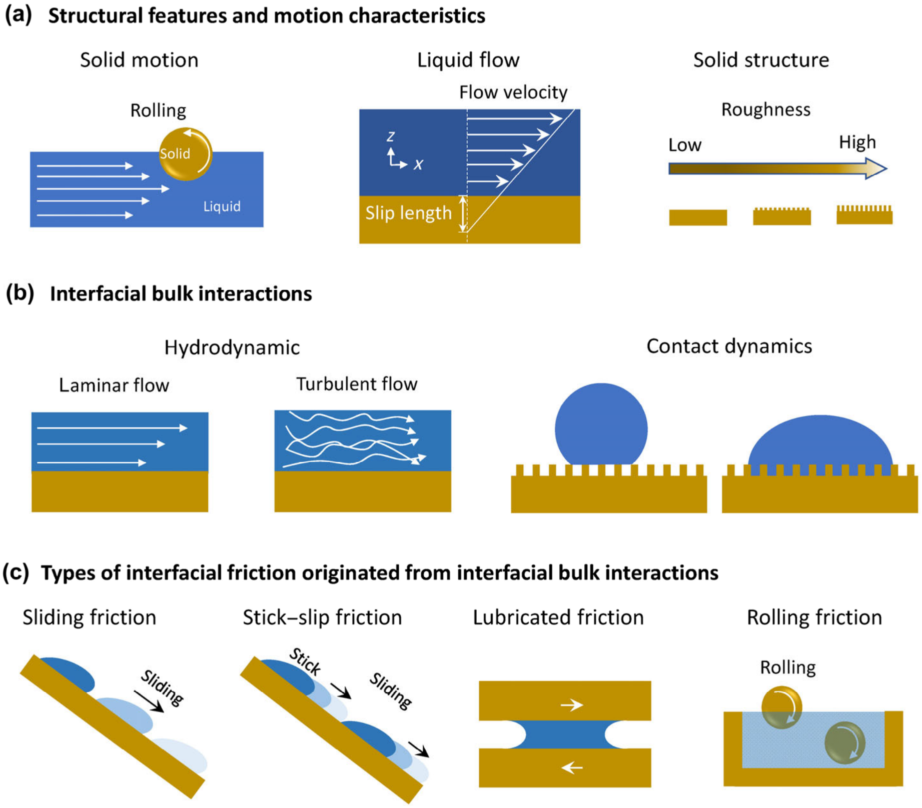

Fig. 3 Interfacial bulk interactions and their related interfacial frictions. (a) Solid and liquid structural features and motion characteristics. (b) Interfacial bulk interactions. (c) Interfacial friction mainly includes sliding, stick–slip, lubricated, and rolling frictions originated from the interfacial bulk interactions.

behaviors of interfacial solids. For instance, lubricated friction [44–50] commonly happens at the interface that a lubricant fluid separates two solid surfaces in relative motions [49, 51–53], e.g., lubrication of machinery [54]. The rolling friction [55, 56] is defined as the force, which resists the rolling motion of a ball or wheel, e.g., particles in liquid [57, 58].

2.2 Interfacial molecular interactions

Different from the interfacial bulk interactions, interfacial molecular interactions originate from the interfacial electromagnetic forces, including physical and chemical interactions, and mainly involve weak intermolecular (such as electrostatic interactions, dipole–dipole interaction, van der Waals force, electric double-layer force, or Casimir force) and strong intramolecular interactions (such as chemical bonding), as shown in Fig. 4(a). These interactions have been accepted as the origin of many interfacial phenomena (Fig. 4(b)), including interface adhesion, interface tension, contact electrification, contact-line pinning, and interfacial chemical reaction. Among them, interface adhesion is a common interfacial phenomenon owing to the interfacial intermolecular attractive force and the transport of liquid viscous action, which is manifested by the molecular interactions between adjacent layers of liquid. Unlike interface adhesion, the interface tension [59–62] origins from cohesive force induced by intermolecular interactions, such as hydrogen bonds or van der Waals

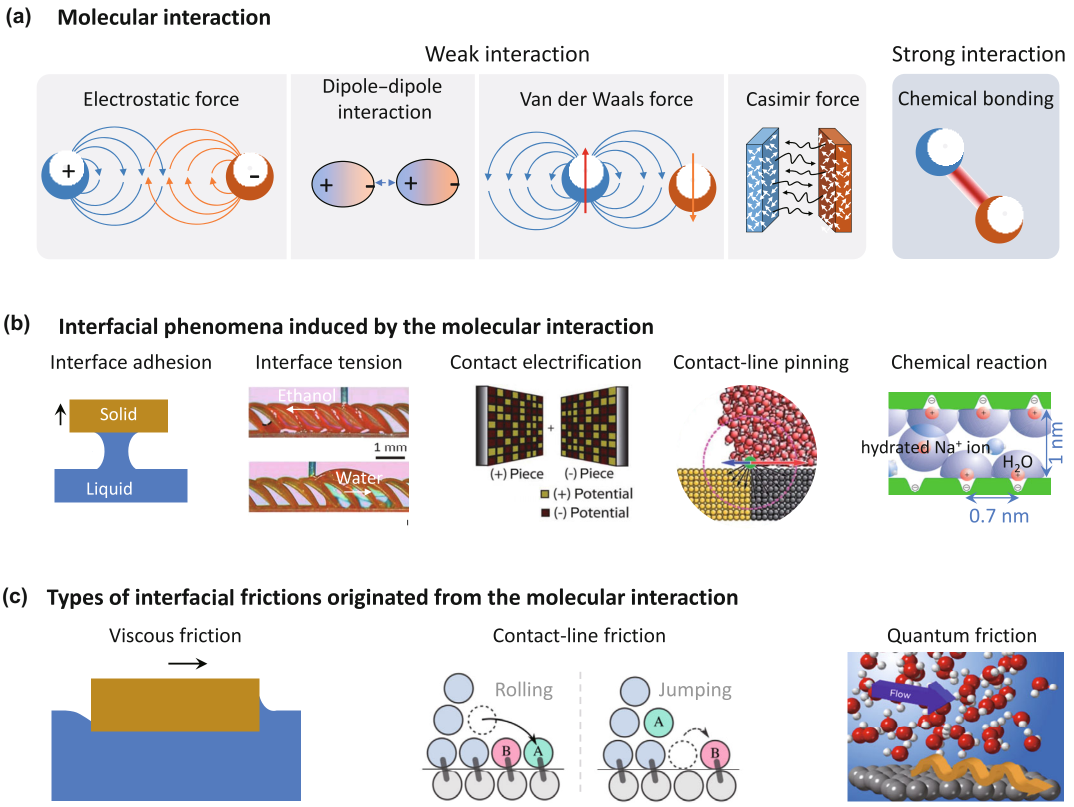

Fig. 4 Interfacial molecular interactions and related interfacial frictions. (a) Main interfacial molecular interactions, possibly including electrostatic interactions, dipole–dipole interaction, van der Waals force, Casimir force, or chemical bonding. (b) Molecular interactions indued interfacial phenomena, including interface adhesion, interface tension, contact electrification, contact-line pinning, or chemical reaction. Reproduced with permission from Ref. [33] for "interface tension", © The Authors 2021; Ref. [69] for "contact electrification", © American Association for the Advancement of Science 2011; Ref. [80] for "contact-line pinning", © The Royal Society of Chemistry 2013; Ref. [82] for "chemical reaction", © The American Association for the Advancement of Science 2002. (c) Interfacial friction mainly includes viscous friction, contact-line friction, and quantum friction from the perspective of the molecular interactions. Reproduced with permission from Ref. [99] for "contact-line friction", © American Physical Society 2018; Refs. [31] for "quantum friction", © The Author(s), under exclusive licence to Springer Nature Limited 2022.

attraction forces between similar molecules. It acts as the key-driven role in the liquid directional steering [33] and the formation of contact angles [63–66]. Additionally, the construction and deconstruction of the interface are always accompanied by charge carrier transfer [67–70] owing to electrostatic interactions or dipole–dipole interactions, which are regarded as the underlying mechanism of interfacial contact electrification [69, 71–75] and electric double layer. In the case of overlapping the double layers between surfaces, the resulting interfacial interaction is often referred to as the electric or electrostatic double-layer force [76], which is important to understand and further regulate wetting, solid–liquid phase separation [77], and other solid–liquid interfacial phenomena. Especially, for DLVO theory [76] about colloidal stability, the electric double-layer force is regarded as one of two fundamental and tradeoff forces except for the van der Waals force. Different from these interactions occurring at single- or two-phase interfaces, the contact-line pinning derived from interface tensions involves solid–liquid–gas three-phase interactions [78–80] and plays critical roles in droplet dynamics at solid surfaces. However, all the above mentioned interfacial interactions are weak. Strong interfacial interactions are still mainly attributed to interfacial chemical bonding [21, 81, 82], such as ionic bonding, covalent bonding, and polar bonding.

Diverse interfacial molecular interactions lead to some distinctive types of interfacial frictions, such as viscous friction, contact-line friction, and quantum friction (Fig. 4(c)). Among them, based on the molecular interactions inside the continuous liquid or at the interfaces with other external matter, the well-known liquid viscosity is manifested by viscous friction that restricts the movement of molecules either within itself or of another medium moving through the liquid [83–85], such as liquid uptake by capillaries [86] and hydrodynamic drag reduction [16, 87, 88]. For the discontinuous liquid, contact-line friction induced by three-phase line pinning [64–66, 89–93] is accepted as one of the main factors restricting the liquid continuous flow behavior [32, 79, 94–98], but the fundamental understanding of the contact line dynamic behaviors remains very limited [93, 99]. Notably, viscous friction and contact-line friction generally act at the contact interfaces. For non-contact interfaces, the interfacial friction is attributed to the non-contact interfacial interactions, such as the Casimir force induced by quantum fluctuations [100, 101]. Thus, quantum friction has been developing as an important supplement for the understanding of these controversial and non-contact interfacial interactions [31, 102–105].

3 Solid–liquid interfacial friction theories

Friction can date back to prehistoric times (before 3500 before Christ (BC)) [24]. The basic theoretical framework of friction was defined by Leonardo da Vinci (1452–1519), who is widely credited with the first quantitative investigations of friction in the 1500s [23–25]. Since that, the past 500 years witness a tremendous development of interfacial friction [26–28], ranging from macroscopic to microscopic, from single-phase interface to multi-phase interface [106] and from contact to non-contact [107–112]. The interfacial friction theory also has significant progress. The initial interfacial friction theory was established at single-phase solid–solid interfaces by investigating the effects of interfacial applied load, contact area, and relative sliding velocity systematically [26–30]. Following by this initial theory, the classical Amontons' law of friction in the 1800s [26–28] consisting of the Amontons' 1st law, the Amontons' 2nd law, and the Coulomb's law [29, 30] is presented and has created a great value for modern industry. Compared to that of solid–solid interfacial friction, the development of solid–liquid interfacial friction is relatively lagging but become more and more important. In Section 3, given the multi-scale properties of the interfacial interaction, we summarize the solid–liquid interfacial friction theories on two research lines, which are based on bulk interactions and molecular interactions.

On the research line of bulk interactions, the study of solid–liquid interfacial friction theory started from confusion by Navier [113] in the 1820s that a thin liquid layer adjacent to a flat surface could exhibit a viscosity with a value quite different from that of the bulk liquid. Furthermore, the theory was developed by Stokes [114] in the 1850s based on the explanation for the origin of the hydrodynamic drag, resulting from aspheric objects with a very low Reynolds number in a viscous liquid. Notably, these theories, which are based on the macroscopic dynamic behaviors of either Amontons' laws of friction or Navier–Stokes fluid theory, are limited to the macroscopic bulk interactions. Despite the continuum description of the bulk flow for water remaining valid down to typically 1 nm [116], the Navier–Stokes equation of the fluid with no-slip boundary condition will fail when liquid–solid friction is low enough [117, 118]. To avoid unacceptable evaluation shifts, some new methods, like the lattice Boltzmann method [119–123], were developed to describe cross-scale interfacial friction behaviors. The lattice Boltzmann method originated from lattice gas automata and discrete particle kinetics utilizing a discrete lattice and discrete time, and is the fusion of the macroscopic kinetic models and the essential physics of microscopic or mesoscopic processes [119].

On the research line of molecular interactions, the interfacial friction theories were started from the molecular theory of friction, based on intermolecular attractive and repulsive force, presented by Tomlinson [124] in the 1920s, and extended to the adhesion theory of friction for static friction by Bowden and Tabor [44, 45, 125] in the 1940s. Then, interfacial friction theories at microscopic have been developed rapidly after the birth of molecular dynamics theory in the 1950s [126]. Diverse molecular dynamics approaches including equilibrium molecular dynamics, non-equilibrium molecular dynamics [127], alternative equilibrium molecular dynamics [128], and *ab initio* molecular dynamics [129] greatly promoted our microscopic fundamental understandings of the interfacial friction [130, 131]. Among them, to obtain highly accurate and high computational efficiency, the linear response method [118, 132–136] based on the equilibrium molecular dynamics [118, 127, 132–136] was presented for the calculation of the solid–liquid interfacial friction. This method starts from the Kubo-like equation [118], and then has been developed into the Green–Kubo relation [134–136]. However, some mechanism of liquid–solid friction remains unknown, with neither current theories nor classical or *ab initio* molecular dynamics simulations. Notably, liquid–solid quantum friction theory has been becoming an important supplement to microscopic interfacial friction theories to reveal some elusive phenomena at extremely confined interfaces [31].

4 Solid–liquid interfacial friction regulation strategies

Fundamentals of interfacial friction have told us how important the interface is. An in-depth understanding of these fundamentals is essential for our exploration of a blueprint for interfacial friction regulation strategies from the perspective of the interface, although there are many developed strategies [137], such as temperature [138–142], pressure [143], electrical [144–148], photo [149, 150], magnetic [151], and vibration [152], for interfacial friction regulation. As we discussed in Section 2, interfacial friction is dominated by interfacial bulk interactions and interfacial molecular interactions, which are closely associated with interfacial dynamic behaviors and types. Therefore, it is reasonable to achieve interfacial friction regulation by tuning the interfacial dynamic behaviors and interfacial types. With this in mind, we summarize the interfacial friction regulation strategies manifested in both natural surfaces and artificial systems, focusing on how liquid, solid, gas, and hydrodynamic coupling mediate the friction.

4.1 Liquid-mediated interfaces

Liquid-mediated interfaces are usually used for dry friction regulation using liquid mediums to transform the interface from solid–solid to solid–liquid. This liquid-mediated strategy has become a well-known friction regulation strategy to reduce the motion resistance or prevent the resultant wear damage. Generally, to ensure that the liquid medium, such as liquid organic matter or water, can reside at the interface for a long time, the liquid medium is constrained in space or on a solid surface. Thus, in Section 4.1, we discuss the liquid-mediated strategies for interfacial friction regulation according to two constraints of liquid medium, including both spatial [153] and surface [95, 154, 155] constraints.

One typical spatial constraint example in biological system [156, 157] is the synovial joint mainly consisting of bones, joint cavity, and synovial fluid, which is constrained in the joint cavity composed of bones [158, 159] (Fig. 5(a)). The constrained synovial fluid is critical to avoiding joint injury and maintaining the long-term mechanical durability of the joint. For spatial constraint, the liquid-mediated interfaces consist of spatial constraint boundaries and the confined liquid medium. The spatial constraint boundaries with different dynamic behaviors dominate the stability of liquid-mediated interfaces. The confined liquid medium acts as a lubricant at the interface. Such a strategy is also evolved in many other biological systems [156, 160], in which the constrained body liquid also acted as the interfacial lubricant to maintain their functional integrity during the whole life with minimized wearing damage. Similarly, the spatial constraint strategy is also widely adopted by artificial systems. Despite the developed liquid mediums being diverse, such as oil [161], ionic liquid [162–166], or solid melting [142, 167–174], the artificial liquid mediums [158, 159, 175–177] are developing to reach an equivalent performance to the biological system. Except for the above-mentioned friend-side effects of these liquid-mediated strategies, liquid-mediated interfacial friction strategies may also lead to some

(a) **Spatial constraint**

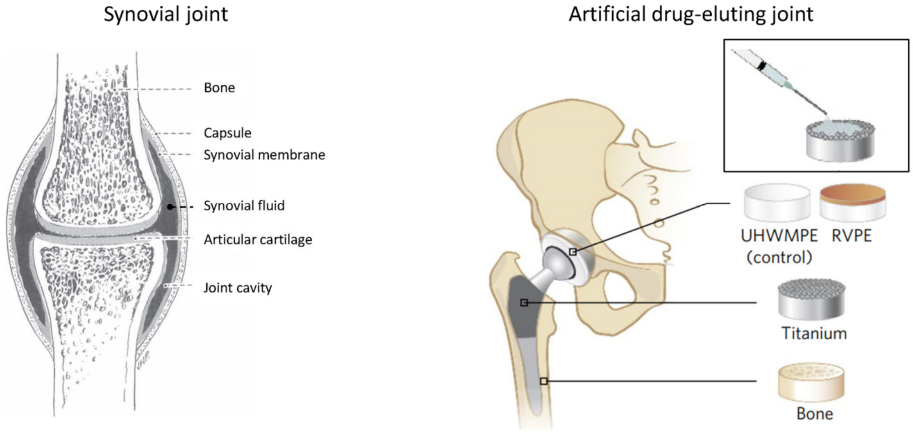

(b) **Surface constraint**

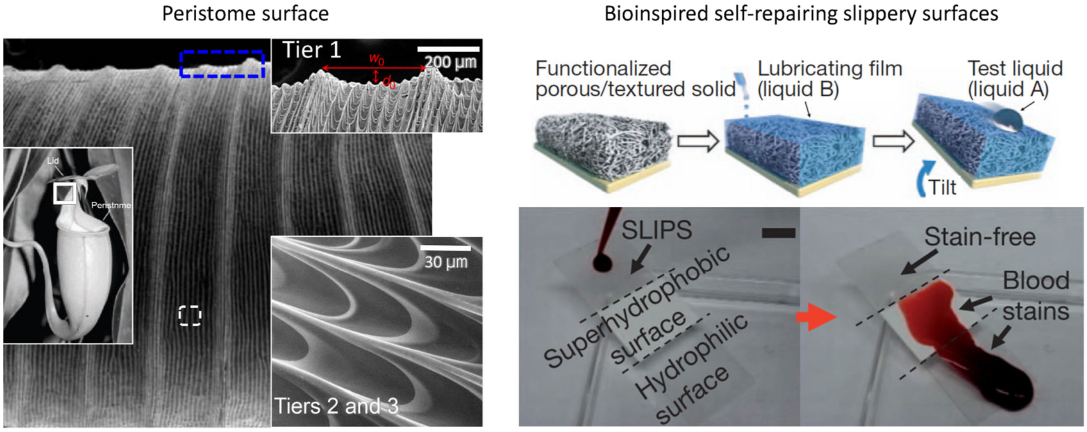

Fig. 5 Liquid-mediated interfacial friction through spatial and surface constraints to maintain the confined liquid. (a) Spatial constraint strategies, such as synovial joint lubrication and artificial drug-eluting joint lubrication. Note: UHWMPE represents ultrahigh molecular weight polyethylene, and RVPE reprensents rifampin-vancomycin-eluting UHMWPE. SLIPS represents slippery liquid-infused porous surface. Reproduced with permission from Ref. [158] for "synovial joint", © IMechE 2007; Ref. [177] for "artificial drug-eluting joint", © Macmillan Publishers Limited, part of Springer Nature 2017. (b) Surface constraint, such as topographical micromorphologies of natural peristome surface and bioinspired self-repairing slippery surfaces. Reproduced with permission from Ref. [155] for the left inset of "peristome surface", © by The National Academy of Sciences of the USA 2004; Ref [181] for the main figure and two right insets of "peristome surface", © The Author(s) 2018; Ref. [95] for "bioinspired self-repairing slippery surfaces", © Macmillan Publishers Limited 2011.

dark-side effects. For example, melted ice-mediated friction of the ice surface causes unstable motion [142, 167–174]. Water-mediated friction of the Longsnout catfish skin greatly reduced by muscle hardening leads to the difficulty of hunting [178]. Also, fluid-mediated faults with low friction properties may cause an unstable movement of the active plate and even leads to an earthquake [179, 180].

Different from spatial constraint, the liquid-mediated interfaces can also be formed on solid surfaces through unique surface engineering or physiochemical interactions. Thus, the liquid-mediated strategies based on surface constraint can be furtherly delivered into two types, including the surface-structured and electromagnetic-force constraints. In terms of the first type, liquid-mediated interfaces, especially liquid mediums, are maintained by the mechanical constraint of the surface structures. For example, a water-mediated low-friction topographical surface [155, 181] (Fig. 5(b)), allowing continuous directional water transport [182–184], has been accepted as the essential reason for insect aquaplaning on the peristome of *Nepenthes* pitcher plants. Inspired by this low-friction topographical surface [182, 183], an artificial liquid-mediated porous surface strategy [95] was successfully demonstrated in anti-fouling. As for the second type, the surface electromagnetic-force constraint mainly originated from physical or chemical interactions. For instance, an ordered water monolayer possibly on the superhydrophilic surface [185–187] has been paid attention to due to its unusual interfacial friction properties that a water droplet on a superhydrophilic surface has a friction coefficient similar to that on a weakly hydrophobic surface.

4.2 Solid-mediated interfaces

Compared with the liquid-mediated interfaces, the solid-mediated interfaces are equipped with a relatively higher stability due to the better constrained ability of the solid medium. Generally, the solid medium can be served as a layer of armor armed on solid or liquid surfaces. Based on the defense objects, the solid-mediated friction regulation strategies can be classified as both besieging solid and besieging liquid.

In the besieging solid strategy, solid-mediated friction regulation strategies focus on the modification of the solid surface using solid mediums, which are discrete particles or solid oil with weak intermolecular interactions but with relatively strong interactions with the besieging solid. Common solid-mediated friction regulation strategy is mainly based on the physical adhesion or adsorption to construct a layer of solid medium on solid surfaces. For example, a hydrophobic wax-mediated leaf surface (Fig. 6(a)) can protect the leaf from injuries of the accumulated pathogens and particulate [188, 189]. Yet, this strategy is inevitably limited by the poor durability in practical applications due to these weak interactions between the solid medium and the defense solid surface. In contrast, artificial chemical coatings on solid surfaces exhibit robust performance due to strong interfacial interactions [190, 191]. For example, an elastomeric flat surface can be tailored using mechanically assembled monolayers to obtain a long-lived superhydrophobic surface [153].

Opposite to the besieging solid strategy, the besieging liquid strategy is relatively rare but also significant for some natural surfaces or practical applications. This approach is mainly achieved by using the additional solids to reduce the contact area between the original interfaces, especially high viscous interfaces. In nature, this approach may be a matter of life and death for some living. For instance, sticky waste disposal of galling aphids is completed by the transformation of interface types from solid–liquid interfaces with high contact area and adhesion to solid–solid interfaces with low contact area and adhesion [192, 193] (Fig. 6(b)). During this process, the interfacial friction experienced a great reduction due to the fundamental reason that the viscous liquid was separated from the body of galling aphids by solid particles, which formed a rough liquid surface and greatly decreased the contact area between the liquid waste and the body of galling aphids. In our lives, these besieging liquid approaches are also common. For example, a stable solid–liquid system, liquid marbles [194, 195], is not difficult to be formed by a liquid droplet on a solid surface with a lot of solid hydrophobic particles [194, 196]. The liquid marble exhibits low friction on the smooth sold substrate due to low contact area and low adhesion

(a) Besieging solid

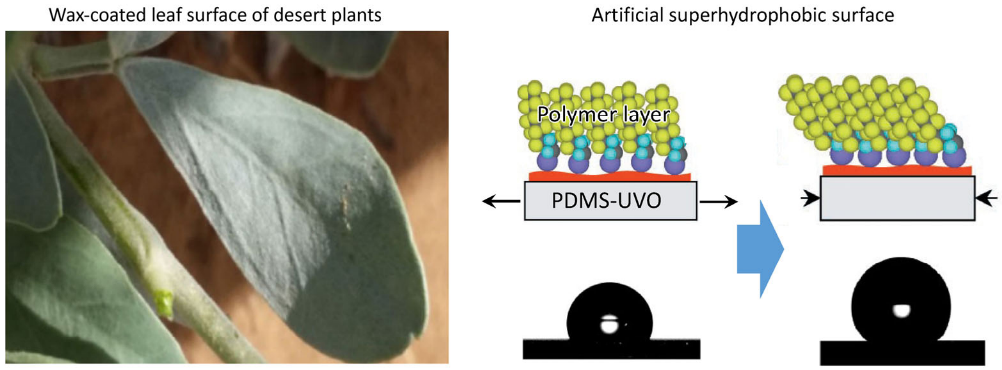

(b) Besieging liquid

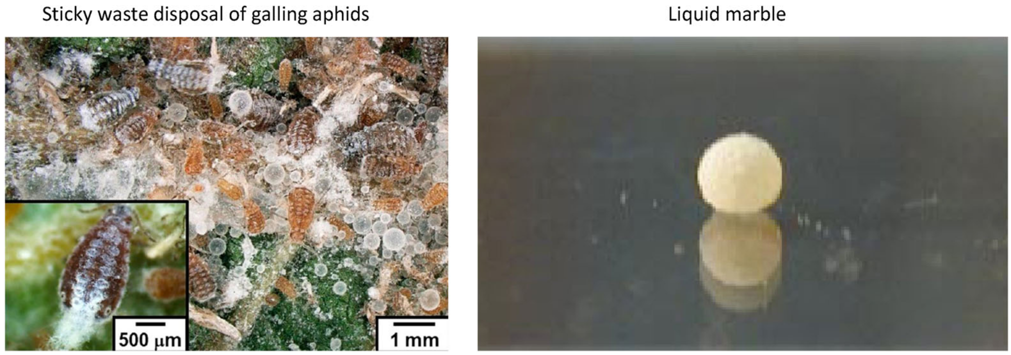

Fig. 6 Solid-mediated interfacial friction through besieging solid or liquid strategies. (a) Besieging solid strategies, such as wax-coated leaf surface of desert plants and poly(dimethylsiloxane) (PDMS) network film polymer surfaces through mechanically assembled monolayers. Note: UVO represents ultraviolet/ozone. Reproduced with permission from Ref. [189] for "wax-coated leaf surface of desert plants", © The author(s) 2015; Ref. [153] for "artificial superhydrophobic surface", © The American Association for the Advancement of Science 2000. (b) Besieging liquid strategies, such as sticky waste disposal of galling aphids and liquid marble. Reproduced with permission from Ref. [193] for "sticky waste disposal of galling aphids", © American Chemical Society 2019; Ref. [197] for "liquid marble", © The Author(s) 2016.

between solid particles on the liquid surface and the solid substrate. Moreover, interfacial friction of liquid marble can sustain the system to stably float on a liquid surface [197], which has been used for evaluating the friction coefficients of the floating marbles based on the dynamic balance of the friction force and capillary force.

4.3 Gas-mediated interfaces

Different from the above-mentioned solid- or liquid-mediated strategies, interfacial friction regulation based on gas/vacuum-mediated interfaces is a spontaneous process in some extremely confined spaces or extreme physical conditions. The spontaneously generated gas bubbles, gas layer, or vacuum is critical to switching the interfacial types or hydrodynamic coupling interactions. Based on the gas/vacuum generated mechanisms, the interfacial friction regulation strategies based on gas/vacuum-mediated interfaces can be classified as the Leidenfrost effect, superhydrophobicity, and cavitation.

Leidenfrost effect [198] is old but still a research hotspot in the field of high-temperature interfacial thermal transfer or dynamics. Interfacial friction regulation by the Leidenfrost effect mainly origins from the generated vapor layer at solid–liquid interfaces [199, 200]. Generally, the vapor layer was created by liquid gasification at high temperatures and became a separatist at the original interfaces to achieve the transformation of interface types from hydrodynamic drag interface to relatively low aerodynamic drag interface. For example, high-velocity droplet transportation on a substrate with a selective Leidenfrost effect [201] can be completed on the ratchet structure surface at high temperatures (Fig. 7(a)) [198, 202, 203], which was mainly attributed to the low interfacial friction by the Leidenfrost effect. Except for the investigations on exploiting the friend side of the Leiddenfrost effect for applications, the dark side of the Leidenfrost effect has become a critical challenge in thermal cooling. To inhibit the Leidenfrost effect at high temperatures, a recently reported rational design of structured thermal armors [5] are successful to inhibit the formation of the vapor layer at 1,150 °C, which is a record performance.

Similar to the Leidenfrost effect, surface superhydrophobicity also introduces gas to regulate interfacial friction. The main difference in surface superhydrophobicity is the way of gas formation that the superhydrophobic surfaces can trap ambient gas based on surface microcavities [8, 204–208]. Leveraging on the trapped gas, superhydrophobicity can regulate

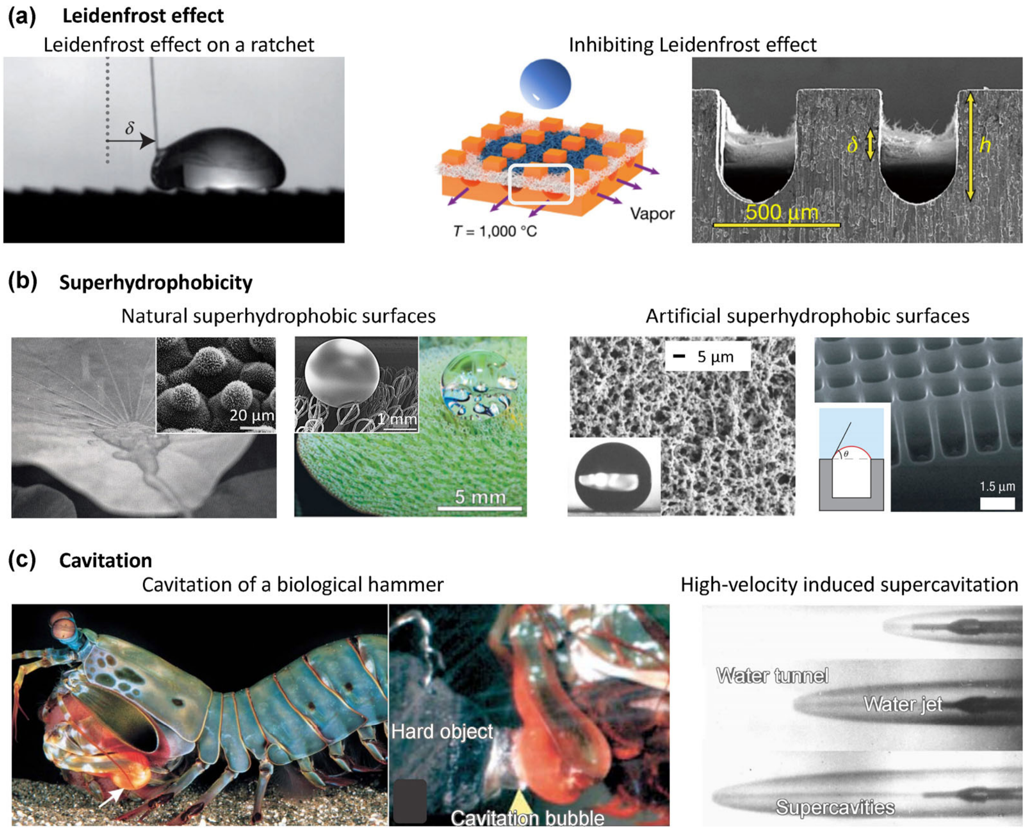

Fig. 7 Gas-mediated interfacial friction through high-temperature induced Leidenfrost effect, microstructured superhydrophobic surface, and high-velocity induced cavitation. (a) Strategies based on Leidenfrost effect, such as Leidenfrost effect on a ratchet and inhibiting Leidenfrost effect. Note: δ, T, and h represent the distance, temperature, and height, respectively. Reproduced with permission from Refs. [203] for "Leidenfrost effect on a ratchet", © Nature Publishing Group 2011; Ref. [5] for "inhibiting Leidenfrost effect", © The Author(s), under exclusive licence to Springer Nature Limited 2022. (b) Strategies based on superhydrophobic surface, such as lotus leaf and micromorphology, *Salvinia* paradox superhydrophobic surface, self-assembled superhydrophobic surface, and micromachined superhydrophobic surface. Note: θ represents the contact angle. Reproduced with permission from Ref. [216] for "lotus leaf" (left figure of "natural superhydrophobic surfaces"), © Klima-und Umweltforschung an der Universität Bonn 1992; Ref. [215] for "its micromorphology" (left inset of "natural superhydrophobic surfaces"), © Springer-Verlag 1997; Ref. [324] for "*Salvinia* paradox superhydrophobic surface" (right figure and inset of "natural superhydrophobic surfaces"), © WILEY-VCH Verlag GmbH & Co. KGaA, Weinheim 2010; Ref. [222] for "self-assembled superhydrophobic surface" (left figure and inset of "artificial superhydrophobic surfaces"), © The American Association for the Advancement of Science 2003; Ref. [210] for "micromachined superhydrophobic surfaces" (right figure and inset of "artificial superhydrophobic surfaces"), © Nature Publishing Group 2007. (c) Strategies based on cavitation, such as cavitation generated by biological hammer impact behavior and supercavitation generated at high-velocity water jet. Reproduced with permission from Ref. [228] for "cavitation of a biological hammer", © The Company of Biologists Limited 2005; Ref. [226] for "high-velocity induced supercavitation", © CaltechCONF 2001.

the interfacial friction by transferring part of solid–liquid interaction to relatively weak solid–gas interaction or mediating the pressure of the trapped gas [209–214]. For instance, it is well known in nature that the self-cleaning mechanism of the lotus leaf (Fig. 7(b)) originated from the microstructured surfaces [215, 216]. To keep the air layer for longer times and under rough conditions typically occurring in turbulent flows, the pinning of the air–water interface at a predefined level by hydrophilic patches is critical. For artificial applications, these nature-inspired microstructured surfaces can be achieved by micromachining [204, 217] and self-assembly [218–221] methods. For example, a porous polypropylene superhydrophobic surface can be obtained by using a suitable selection of solvents and temperatures [222] (Fig. 7(b)). Compared to the self-assembled methods, the micromachining patterned superhydrophobic surfaces are better controllable, so it is possible to turn the interfacial friction from lubrication to anti-lubrication through high-precise changing the liquid–gas menisci of the trapped gas [210]. To enhance the mechanical stability, natural superhydrophobic surfaces also provide us with more feasible solutions, such as *Salvinia*-like slippery surface [223] and springtail-inspired superomniphobic surface [224, 225], even for some extreme conditions.

Compared to the first two strategies, cavitation is also based on vapor but is relatively rare. The vapor is obtained by a high-velocity body traveling through the liquid [226, 227]. For instance, an extreme impact of the peacock mantis shrimp [228] can generate cavitation by a high-velocity moving hammer under low fluid friction (Fig. 7(c)). Due to the interface transfer from solid–liquid to solid–gas, cavitation is promising to obtain ultra-low interfacial friction, which is a benefit for achieving high-velocity movement in liquid. This idea evoked broad investigation on cavitation due to its great potential for high-velocity underwater weapons. To leverage this strategy at low-velocity sceneries, artificial cavitation methods, such as adding bubbles or ejecting air/gas [209–212], also drive rapid development. Furthermore, supercavitation, as the use of a cavitation bubble to drag reduction, is being developed as a critical technique for high-velocity underwater vessel [226].

4.4 Hydrodynamic coupling-mediated interfaces

In striking contrast to the usage of the phase (liquid, gas, and solid)-mediated interfaces, hydrodynamic coupling-mediated interfaces take advantage of inherent mechanical coupling interaction rather than the transformation of interface types based on the generated, trapped, or added liquid, solid, or gas. In Section 4.4, based on the driving types of the mechanical coupling interaction, the hydrodynamic coupling-mediated strategies can be classified as passive and active strategies.

The passive strategies are widely used for our practical applications and rely on numerous energy consumption to maintain. Based on mechanical coupling interaction, the passive friction regulation strategies mainly rely on the liquid flow characteristics, relative motion characteristics, and external stimuli. Among them, liquid flow characteristics and relative motion characteristics are predicted by Navier–Stokes equation [229–233] and Newtonian mechanics or dynamics, respectively. Unlike the solid or liquid dynamic characteristics, the external stimuli, such as temperature [138–142, 234–238], pressure [143], electrical [144–146, 239–242], photo [149, 150], magnetic [151], and vibration [152], mainly take advantage of the sensitive characteristics of the interfacial intrinsic properties to affect the mechanical coupling interaction. For example, through low interfacial friction property of shark skin has been well-known attributed to the three-dimensional microstructured rib pattern, the imparted streamwise vortices at interfaces, which relies on Refs. [18, 243, 244] (Fig. 8(a)). However, this skin interfacial friction is known to reduce in the external turbulent-flow regime [244]. Even for a fully flexible biomimetic shark skin [245], the performance of friction regulation remains in close relationship with special motion behaviors.

Different from passive strategies, active strategies for interfacial friction regulation do not suffer from additional energy consumption, which is unexpected for green or low-carbon development. For the active strategies, the interfacial friction is mainly balanced by the interfacial forces, such as capillary force, gradient force of surface, gravity, and electrostatic force. Typically, common interface tension-induced capillary flow [246] could balance the fluid viscous friction and contact-line friction to achieve spontaneous liquid flows, such as water transport in plant vessels [6], slippery ventral skin of *Lampropeltis pyromelana* [247], and droplet uphill [248]. In addition, these actively spontaneous liquid flows are also affected by the liquid inherent characteristics, such as liquid directional steering in the *Araucaria* leaf structure [33] (Fig. 8(b)). Similar approaches have been developed in the artificial system to construct a liquid rectifier for liquid flow control. For example, nature-inspired liquid diodes [20, 183, 249–253] relying on capillary force regulate the transport of liquids spontaneously. Or a programmed droplet transport with high velocity relies on the surface charge density gradients [242].

5 Applications

Interfacial friction mainly involves two sides of applications: From the perspective of the bright side, interfacial friction can obtain interfacial mass and energy transfer for surface cleaning, energy harvesting, or liquid harvesting. From the other perspective of the dark side, friction causes energy loss, surface wearing, or surface corrosion [254]. Considering both sides of the interfacial friction in certain applications, we summarize the applications of interfacial friction from two classifications: friction-inhibited and friction-reinforced applications.

5.1 Interfacial friction-inhibited applications

In friction-inhibited applications, the interfacial

(a) Passive mediation

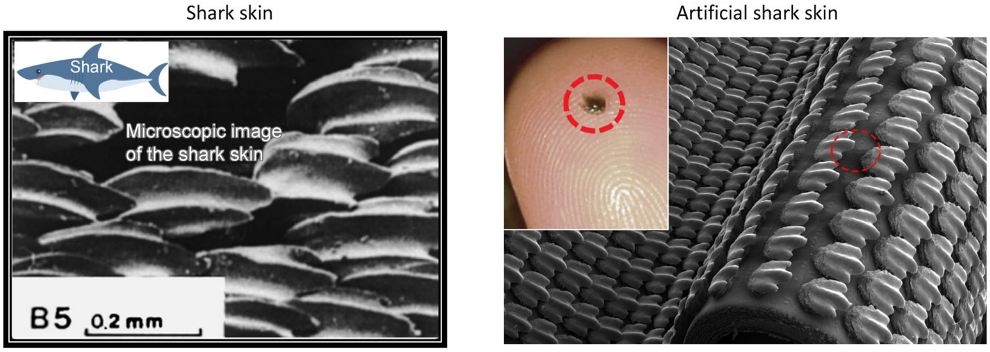

(b) Active mediation

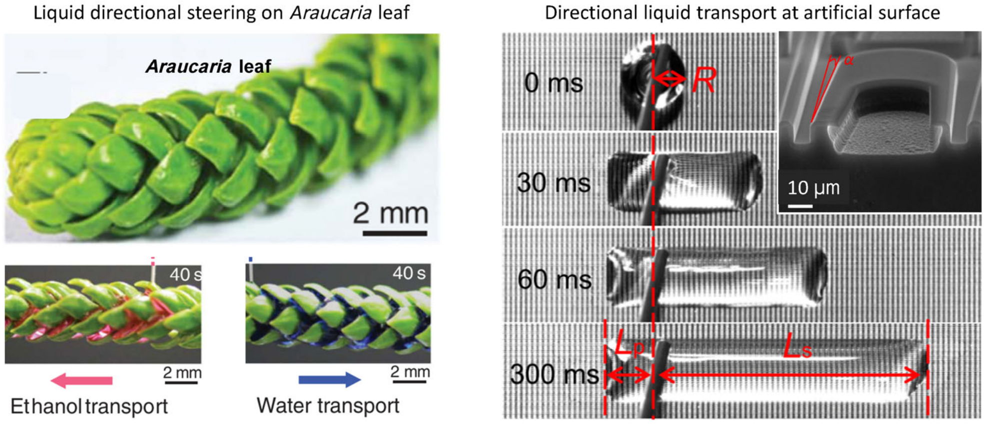

Fig. 8 Hydrodynamic coupling-mediated interfaces through passive and active strategies. (a) Passive-mediated strategies, such as drag reduction of shark skin and flexible biomimetic shark skin. Reproduced with permission from Ref. [243] for "shark skin", © Springer-Verlag 2000; Ref. [245] for "artificial shark skin", © Published by The Company of Biologists Ltd 2014. (b) Active-mediated strategies, such as liquid directional steering on *Araucaria* leaf and topological liquid diode. Note: R, L_p, L_s, and α represent the radius, droplet in the major spreading direction, droplet in the pinning direction, and apex angle of the diverging side-channel, respectively. Reproduced with permission from Ref. [33] for "liquid directional steering on *Araucaria* leaf", © The Authors 2021; Ref. [252] for "directional liquid transport at artificial surface", © The Authors 2017.

friction is expected to be reduced as much as possible through interfacial mediations, which can break the contact-line pinning, overcome the liquid viscous resistance, or transfer the interface interaction from strong to weak. Main friction-inhibited applications include three aspects, which are drag reduction, anti-wearing, and anti-fouling (Fig. 9(a)).

Drag reduction is the most important application in investigating interfacial friction regulation strategies due to the tremendous economic cost resulting from the huge shipping [255] each year and the vast networks of pipes crisscrossing our cities globally [256]. Drag reduction mainly lies in achieving low-energy consumption for solid or liquid medium transport and pipeline flow [256–261]. In terms of solid transport, drag reduction is mainly achieved by compliant surface coating, interface type switching from high friction to low friction, and structural design by hydrodynamics, such as common bulb bow design and air/gas layer construction [255, 262, 263] in ships or underwater vehicles. Considering the liquid transport, drag reduction in pipes mainly relies on the adjustment of the fluid viscosity [257], Reynolds number [256], and the relative roughness of the inwall [229–233] based on the hydrodynamics and traditional friction laws. However, these friction correlations at the macroscale may not apply to micro/nanoscale scenarios [264, 265]. Friction in micro/nanochannels with a large surface-to-volume ratio performs more sensitive-to-surface properties [266–268]. Exploring size-dependent solid–liquid interfacial friction in micro/nanochannels has become a research hotspot due to unexpected water- and ion-transport phenomena [269–272], such as electronic friction from the inwall [273–275], water thermophoresis [276], phonon-induced oscillating friction [277], and fast water transport [130, 278]. Following these explorations, developing effective drag reduction in micro/nanochannel is also very significant. Currently, lots of the corresponding approaches, such as superhydrophobic surfaces [266, 279, 280], surfactant [281], microchannel cross-section shape [282, 283], capillary-condensed water [284, 285], and some strategies to reduce the liquid viscosity [286], have been presented and will play a key role in micro-/nano-fluidic applications. More efforts still need to be made for their practical applications.

Different from drag reduction, anti-wearing mainly

(a) Friction-inhibited applications

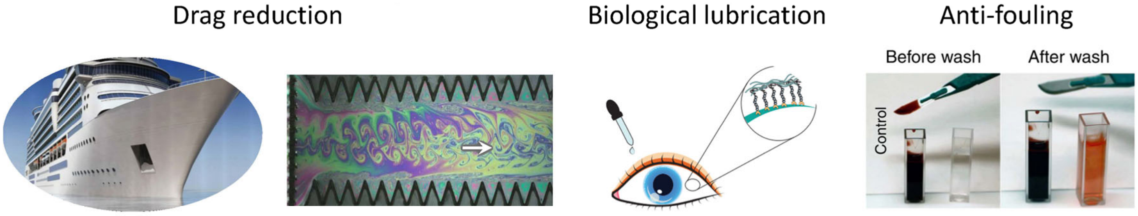

(b) Friction-reinforced applications

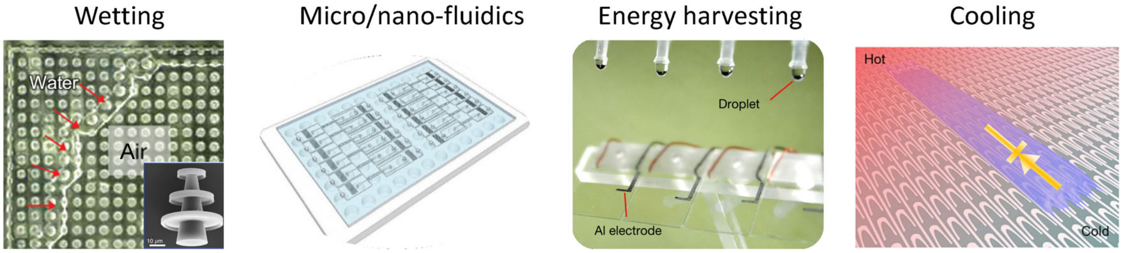

Fig. 9 Representative applications of interfacial friction. (a) Friction-inhibited applications, such as drag reduction, biological lubrication, and anti-fouling. Reproduced with permission from Ref. [261] for "drag reduction", © American Association for the Advancement of Science 2021; Ref. [12] for "biological lubrication", © Macmillan Publishers Limited 2014; Ref. [287] for "anti-fouling", © Macmillan Publishers Limited 2015. (b) Friction-reinforced applications, such as wetting, micro-/nano-fluidics, energy harvesting, and cooling. Reproduced with permission from Ref. [255] for "wetting", © AIP Publishing 2021; Ref. [115] for "micro-/nano-fluidics", © The Royal Society of Chemistry 2017; Ref. [3] for "energy harvesting", © The Author(s), under exclusive licence to Springer Nature Limited 2020; Ref. [20] for "cooling", © American Chemical Society 2021.

focuses on preventing mass transfer in the process of interfacial friction. Anti-wearing mainly involves the durability of machinery [54] and artificial bio-devices or implants in biological systems. To achieve anti-wearing, solid- or liquid-mediated interfacial friction regulated strategies are common in practical applications. For example, a polymer–peptide surface coating is potential to treat tissue-lubricating dysfunction [12]. Remarkably, mimicking these biological systems has been a promising anti-wearing approach to obtaining an efficient and durable engineering system for the rehabilitation of disabled people or industrial applications.

Except for the widely concerned drag reduction and anti-wearing, anti-fouling has also been gradually paid more attention in many recent applications. In anti-fouling, the friction inhabitation as much as possible is a benefit to obtain a low surface adhesion for easy falling off the contaminants [287]. At present, anti-fouling is a major challenge in marine engineering equipment and medical settings [14, 15]. For the marine engineering equipment, the formed biofouling film can accumulate on the surfaces followed by the attachment of larger marine organisms and greatly increases the fuel burn of seafaring vessels [288]. The movement of biofouling film is generally achieved by hydrodynamic coupling-mediated strategies, such as high-velocity water shearing. The faced challenge is that most marine engineering equipment works at a quasi-static state, which needs to pay additional energy consumption for the hydrodynamic coupling-mediated strategies. Recently, gas-mediated strategies were paid more attention to solving the challenges in these applications and were expected to achieve a combinative effect on both drag reduction and anti-fouling. In medical settings, biofouling may cause persistent infections through blood or body liquid. To ensure the robustness of the solid surface, current anti-fouling mainly relies on strong chemical bonding strategies to obtain low friction. However, chemical coatings may cause secondary pollution to the liquid, which is not preferred for the environment or health. Therefore, robust superhydrophobic surface, such as armor-defense nature-inspired design [225, 289, 290], has been presented as the potential solution for this question.

5.2 Interfacial friction-reinforced applications

Except for the dark side in friction-inhibited applications, interfacial friction also has a bright side and can reinforce the interfacial properties in some practical applications, if the friction process with energy and mass transfer is reasonably leveraged. According to the fundamental physical processes of interfacial friction, the developed friction-reinforced applications (Fig. 9(b)) are mainly classified into three types based on the various frictional functions, including interfacial interactive force, charge carrier transfer, and energy dissipation.

Leveraging on the friction-induced interfacial interactive force, it is expected to obtain high-precise liquid operation [21, 22], perfect surface wetting performance [8, 9], high-performance micro-/nano-fluidic devices [115], and efficient liquid harvesting [19]. In terms of liquid operation, well controlling and employing the liquid viscous friction is essential to obtaining precise droplet generation, high-efficient liquid flow, and sufficient mixing, which are critical for printing technology, heat management, and chemical reactions. Unlike liquid operation, wetting as a three-phase interfacial dynamic process mainly lies in the force balance between adhesive and cohesive forces, which can be regulated by surface topography [8, 9] or surface tensions. Thus, wetting is significant in the bonding or adherence of two materials. As for the micro-/nano-fluidics, interfacial friction can provide an expected balance force to control the fluid flow behavior [6, 7]. To well balance the interfacial friction, numerous approaches were presented, mainly including external mediation approaches, temperature [138–142], pressure [143], electrical [144–148], photo [149, 150], magnetic [151], and vibration [152], and internal mediation approaches, such as liquid pH [291], ionic liquid lubricants [162–166], bubble additives [209–212], the conformation of the surface polymers [292], and surface molecular shape [293]. Generally, these external mediation approaches are with better controllability and flexibility than the internal one. Besides, it has been accepted that the water collection efficiency from vapor is limited by the intrinsic trade-off between fast droplet nucleation and efficient droplet removal [10, 11]. Low interfacial friction is promising to provide a low adhesion surface and effectively decouple the inherent trade-off [10] so that the droplet can easily move and collect.

Except for the interfacial interactive force, the frictional process is accompanied by charge carrier transfer at the interfaces. Leveraging on the friction-induced interfacial charge carrier transfer, interfacial friction regulation is promising to improve the performance in interfacial energy harvesting [3, 294–298] and sensing [299]. Fundamentally, high-efficiency interfacial charge carrier transfer is essential for a high-performance solid–liquid energy harvester or sensor. However, the interfacial friction regulation faces a fundamental challenge of the trade-off between a large interfacial contact area and contact time as short as possible. Recently, a droplet-based electricity generator performs excellent electrical energy output and may be potential to overcome this concern by using the impinged water droplet for large contact area and the liquid slippery polytetrafluoroethylene surface for droplet fast slipping [3].

As is known, friction is always accompanied by energy dissipation. Leveraging on the intrinsic energy dissipation, the interfacial friction could be used for collecting or transferring some undesired energy at the surface, such as chaotic motion stabilizing and thermal cooling. However, under some extreme conditions, achieving this process faces giant challenges, such as low-efficiency thermal cooling at high temperatures due to the limitation of the Leidenfrost effect, which creates a gas-mediated interface to get an ultralow friction property. To inhibit the Leidenfrost effect, the gas should be removed at a high temperature for the achievement of the high friction property. Recently, a rational design of structured thermal armors was presented for efficient cooling at 1,150 °C [5]. The gas was evacuated by U-shaped channels to skillfully modulate the interfacial friction for efficient interfacial energy transfer during full contact.

6 Summary and challenges

Interfacial friction is essential to revealing almost all interface-related natural phenomena or achieving high-efficiency and high-performance industrial applications. Fundamental understanding and flexible regulation strategies of interfacial friction are significant for many key applications. This review provides a timely summary of interfacial friction interaction and regulation strategies from the perspectives of interfaces, including liquid-, gas-, solid-, and hydrodynamic coupling-mediated interfaces. Meanwhile, this review also highlights both sides of interfacial friction and some representative applications.

Despite great advances in friction that have been created, many fascinating friction problems, such as the origin of friction [31, 52, 81, 99, 102, 300, 301] and some counterintuitive phenomena in extremely confined boundary [107–112], still occupy a key position in the current research owing to their massive impact on various areas [302]. The origin of interfacial friction remains elusive involving contact electrification, contact line moving mechanism, and interfacial quantum interactions. In terms of contact electrification, Refs. [303–305] have demonstrated that interfacial contact electrification has both electron transfer and ion transfer. However, it is not clear who plays a dominant role in this process and whether there are some other unknown mass or energy transfers in this process. In the aspect of contact-line moving, many theoretical models and proposals have been developed for resolving the incompatibility with the nonslip boundary condition over the past years [9, 93, 306–309], but experimentally verifications are challenging. As for interfacial quantum interactions, despite remarkable and exciting progress over the past decade, some controversial sounds remain. It is unknown whether the interfacial quantum friction theory on account of water–carbon interfaces is suitable for revealing some other counterintuitive phenomena at other extremely confined interfaces [269, 310]. Besides, some interfacial friction behaviors in the extremely confined boundary are intriguing and counterintuitive. For instance, superhydrophobic surfaces with multi-level structures would not only reduce friction in liquid flows under pressure but also enable directional control of the slip [311]. Transistor-like electrohydrodynamic effect can be found in molecular-sized slit-like channels [269] using two-dimensional materials [130, 278], such as graphene [312–317], hexagonal boron nitride (hBN) [129, 318–320], MoS_2 [321, 322], and atomically-smooth α-Fe(100) slabs [143].

Fundamentally understanding the interfacial friction is essential to achieving well interfacial friction regulation. The available interfacial friction regulation strategies refer to solid surface morphology, liquid characteristics, environmental stimuli, and structural dynamic behaviors. Obtaining desired interfacial friction still faces some key challenges, especially inhibition of the interfacial friction and dynamic tunability of friction properties. In terms of inhibiting interfacial friction, the development of drag reduction seems to have reached a limit based on traditional approaches mainly involving solid- and liquid-mediated strategies. The combination of gas phase may provide a significant improvement in current drag reduction because aerodynamic drag is very small in comparison to hydrodynamic drag. This is the partial reason why superhydrophobic surfaces can get a considerable effect on interfacial friction. However, most of these solid surfaces are fabricated with a fragile micro/nanostructure of materials to date, which calls for more novel designs and fabrication processes to improve this concern.

Additionally, interfacial friction regulation in anti-wearing and anti-fouling encounters a great challenge that how to maintain long-term stability and mechanical reliability of the lubrication and low surface energy coating. In contrast, interfacial friction regulation in energy harvesting and cooling is also difficult to achieve high-efficient energy conversion and mass transfer. As for wetting and micro-/nano-fluidic, how to provide custom friction is critical in practical applications. Besides, obtaining the dynamic tunability of the interfacial friction is interesting and promising for greatly broadening the surface function by the fusion of smart materials [151, 323] or structures [242] and advanced actuating approaches.

Acknowledgements

This work was supported by the funding from Health@InnoHK (Hong Kong Centre for Cerebro–cardiovascular Health Engineering (COCHE)), the Innovation and Technology Commission, the Government of the Hong Kong Special Administrative Region of the People's Republic of China, the National Natural Science Foundation of China (12102250), and China Postdoctoral Science Foundation (2020TQ0190 and 2020M681290).

Declaration of competing interest

The authors have no competing interests to declare that are relevant to the content of this article.

References

[1] He Y, She D S, Liu Z Y, Wang X, Zhong L, Wang C M, Wang G F, Mao S X. Atomistic observation on diffusion-mediated friction between single-asperity contacts. *Nat Mater* **21**(2): 173–180 (2022)

[2] Kessler D A. Surface physics—A new crack at friction. *Nature* **413**(6853): 260–261 (2001)

[3] Xu W H, Zheng H X, Liu Y, Zhou X F, Zhang C, Song Y X, Deng X, Leung M, Yang Z B, Xu R X, et al. A droplet-based electricity generator with high instantaneous power density. *Nature* **578**(7795): 392–396 (2020)

[4] Wu H, Mendel N, van den Ende D, Zhou G F, Mugele F. Energy harvesting from drops impacting onto charged surfaces. *Phys Rev Lett* **125**(7): 078301 (2020)

[5] Jiang M N, Wang Y, Liu F Y, Du H H, Li Y C, Zhang H H, To S, Wang S, Pan C, Yu J H, et al. Inhibiting the Leidenfrost effect above 1,000 °C for sustained thermal cooling. *Nature* **601**(7894): 568–572 (2022)

[6] Dudukovic N A, Fong E J, Gemeda H B, DeOtte J R, Cerón M R, Moran B D, Davis J T, Baker S E, Duoss E B. Cellular fluidics. *Nature* **595**(7865): 58–65 (2021)

[7] Zhang Z, Wen L P, Jiang L. Nanofluidics for osmotic energy conversion. *Nat Rev Mater* **6**(7): 622–639 (2021)

[8] Joly L, Biben T. Wetting and friction on superoleophobic surfaces. *Soft Matter* **5**(13): 2549–2557 (2009)

[9] Quéré D. Wetting and roughness. *Annu Rev Mater Res* **38**: 71–99 (2008)

[10] Wang X K, Zeng J, Li J, Yu X Q, Wang Z K, Zhang Y F. Beetle and cactus-inspired surface endows continuous and directional droplet jumping for efficient water harvesting. *J Mater Chem A* **9**(3): 1507–1516 (2021)

[11] Zheng Y M, Bai H, Huang Z B, Tian X L, Nie F Q, Zhao Y, Zhai J, Jiang L. Directional water collection on wetted spider silk. *Nature* **463**(7281): 640–643 (2010)

[12] Singh A, Corvelli M, Unterman S A, Wepasnick K A, McDonnell P, Elisseeff J H. Enhanced lubrication on tissue and biomaterial surfaces through peptide-mediated binding of hyaluronic acid. *Nat Mater* **13**(10): 988–995 (2014)

[13] Bodega F, Sironi C, Porta C, Zocchi L, Agostoni E. Pleural liquid and kinetic friction coefficient of mesothelium after mechanical ventilation. *Resp Physiol Neurobi* **206**: 1–3 (2015)

[14] Chen S F, Jiang S Y. A new avenue to nonfouling materials. *Adv Mater* **20**(2): 335–338 (2008)

[15] Yang J T, Chen H, Xiao S W, Shen M X, Chen F, Fan P, Zhong M Q, Zheng J. Salt-responsive zwitterionic polymer brushes with tunable friction and antifouling properties. *Langmuir* **31**(33): 9125–9133 (2015)

[16] Driels M R, Ayyash S. Drag reduction in laminar flow. *Nature* **259**(5542): 389–390 (1976)

[17] Radin I, Zakin J L, Patterson G K. Drag reduction in solid-fluid systems. *AIChE J* **21**(2): 358–371 (1975)

[18] Bechert D W, Hoppe G, Reif W E. On the drag reduction of the shark skin. In: Proceedings of the 23rd Aerospace Sciences Meeting, Reno, NV, USA, 1985: 546.

[19] Lv P, Zhang Y L, Han D D, Sun H B. Directional droplet transport on functional surfaces with superwettabilities. *Adv Mater Interfaces* **8**(12): 2100043 (2021)

[20] Li J Q, Zhou X F, Tao R, Zheng H X, Wang Z K. Directional liquid transport from the cold region to the hot region on a topological surface. *Langmuir* **37**(16): 5059–5065 (2021)

[21] Joly L, Tocci G, Merabia S, Michaelides A. Strong coupling between nanofluidic transport and interfacial chemistry: How defect reactivity controls liquid–solid friction through hydrogen bonding. *J Phys Chem Lett* **7**(7): 1381–1386 (2016)

[22] Zhao L, Sun J J, Wang X, Zeng L, Wang C L, Tu Y S. System-size effect on the friction at liquid–solid interfaces. *Appl Math Mech-Engl* **41**(3): 471–478 (2020)

[23] Mo Y F, Turner K T, Szlufarska I. Friction laws at the nanoscale. *Nature* **457**(7233): 1116–1119 (2009)

[24] Dowson D. *History of Tribology*. Reading (USA): Addison–Wesley Longman Ltd, 1979.

[25] Hutchings I M. Leonardo da Vinci's studies of friction. *Wear* **360–361**: 51–66 (2016)

[26] Dowson D. Men of tribology: Guillaume Amontons (1663–1705) and John Theophilus Desaguliers (1683–1744). *J Lubr Technol* **100**(1): 2–5 (1978)

[27] Amontons G. De la resistance cause'e dans les machines (about resistance and force in machines). *Mem l'Acedemie R A*: 257–282 (1699)

[28] Popova E, Popov V L. The research works of Coulomb and Amontons and generalized laws of friction. *Friction* **3**(2): 183–190 (2015)

[29] Heyman J. *Coulomb's Memoir on Statics: An Essay in the History of Civil Engineering*. Cambridge (UK): Cambridge University Press, 1972.

[30] Coulomb C A. Essai sur une application des regles de maximis et minimis quelques problemes de statique, relatits a l'architecture. *Memoires de Mathematique de l'Academie Royale de Science* **7**: 343–382 (1773) (in French)

[31] Kavokine N, Bocquet M L, Bocquet L. Fluctuation-induced quantum friction in nanoscale water flows. *Nature* **602**(7895): 84–90 (2022)

[32] Mouterde T, Raux P S, Clanet C, Quéré D. Superhydrophobic frictions. *PNAS* **116**(17): 8220–8223 (2019)

[33] Feng S L, Zhu P G, Zheng H X, Zhan H Y, Chen C, Li J Q, Wang L Q, Yao X, Liu Y H, Wang Z K. Three-dimensional capillary ratchet-induced liquid directional steering. *Science* **373**(6561): 1344–1348 (2021)

[34] Zhang Newby B M, Chaudhury M K. Friction in adhesion. *Langmuir* **14**(17): 4865–4872 (1998)

[35] McFarlane J S, Tabor D. Relation between friction and adhesion. *P Roy Soc A-Math Phy* **202**(1069): 244–253 (1950)

[36] Xiao F, Chen Z, Wei Z X, Tian L L. Hydrophobic interaction: A promising driving force for the biomedical applications of nucleic acids. *Adv Sci* **7**(16): 2001048 (2020)

[37] Ballauff M. More friction for polyelectrolyte brushes—Trivalent yttrium cations increase friction greatly compared with monovalent cations. *Science* **360**(6396): 1399–1400 (2018)

[38] Cottin-Bizonne C, Cross B, Steinberger A, Charlaix E. Boundary slip on smooth hydrophobic surfaces: Intrinsic effects and possible artifacts. *Phys Rev Lett* **94**(5): 056102 (2005)

[39] Ma M D, Shen L M, Sheridan J, Liu J Z, Chen C, Zheng Q S. Friction of water slipping in carbon nanotubes. *Phys Rev E* **83**(3): 036316 (2011)

[40] Brigo L, Natali M, Pierno M, Mammano F, Sada C, Fois G, Pozzato A, dal Zilio S, Tormen M, Mistura G. Water slip and friction at a solid surface. *J Phys Condens Matter* **20**(35): 354016 (2008)

[41] Aranson I S, Tsimring L S, Vinokur V M. Stick–slip friction and nucleation dynamics of ultrathin liquid films. *Phys Rev B* **65**(12): 125402 (2002)

[42] Lei Y J, Leng Y S. Stick–slip friction and energy dissipation in boundary lubrication. *Phys Rev Lett* **107**(14): 147801 (2011)

[43] Balzer B N, Gallei M, Hauf M V, Stallhofer M, Wiegleb L, Holleitner A, Rehahn M, Hugel T. Nanoscale friction mechanisms at solid–liquid interfaces. *Angew Chem Int Ed* **52**(25): 6541–6544 (2013)

[44] Bowden F P, Gregory J N, Tabor D. Lubrication of metal surfaces by fatty acids. *Nature* **156**(3952): 97–101 (1945)

[45] Bowden F P, Moore A J W. Adhesion of lubricated metals. *Nature* **155**(3937): 451–452 (1945)

[46] Bowden F P, Tabor D. Friction, lubrication and wear: A survey of work during the last decade. *Brit J Appl Phys* **17**(12): 1521–1544 (1966)

[47] Kalin M, Polajnar M. The effect of wetting and surface energy on the friction and slip in oil-lubricated contacts. *Tribol Lett* **52**(2): 185–194 (2013)

[48] Tang, J Z, Ding, Q, Hu, L T, Qin, B F. Effects of viscosity, polarity and friction pairs on the friction behavior of lubricated DLC film. *Tribology* **34**(2): 180–186 (2014) (in Chinese)

[49] Cafolla C, Foster W, Voïtchovsky K. Lubricated friction around nanodefects. *Sci Adv* **6**(14): eaaz3673 (2020)

[50] Cheikh C, Koper G. Friction in surfactant layers at solid–liquid interfaces. *Colloid Surface A* **270–271**: 252–256 (2005)

[51] Holmberg K, Erdemir A. Influence of tribology on global energy consumption, costs and emissions. *Friction* **5**(3): 263–284 (2017)

[52] Ma L R, Gaisinskaya-Kipnis A, Kampf N, Klein J. Origins of hydration lubrication. *Nat Commun* **6**: 6060 (2015)

[53] Dhopatkar N, Defante A P, Dhinojwala A. Ice-like water supports hydration forces and eases sliding friction. *Sci Adv* **2**(8): e1600763 (2016)

[54] Veltkamp B, Velikov K P, Venner C H, Bonn D. Lubricated friction and the Hersey number. *Phys Rev Lett* **126**(4): 044301 (2021)

[55] Briggs G A D, Briscoe B J. Effect of surface roughness on rolling friction and adhesion between elastic solids. *Nature* **260**(5549): 313–315 (1976)

[56] Lee W G, Cho K H, Jang H. Molecular dynamics simulation of rolling friction using nanosize spheres. *Tribol Lett* **33**(1): 37–43 (2009)

[57] Blais B, Bertrand F. CFD-DEM investigation of viscous solid–liquid mixing: Impact of particle properties and mixer characteristics. *Chem Eng Res Des* **118**: 270–285 (2017)

[58] Perrin H, Clavaud C, Wyart M, Metzger B, Forterre Y. Interparticle friction leads to nonmonotonic flow curves and hysteresis in viscous suspensions. *Phys Rev X* **9**(3): 031027 (2019)

[59] Roy P, Liu S H, Dutcher C S. Droplet interfacial tensions and phase transitions measured in microfluidic channels. *Annu Rev Phys Chem* **72**(1): 73–97 (2021)

[60] Zarzar L D, Sresht V, Sletten E M, Kalow J A, Blankschtein D, Swager T M. Dynamically reconfigurable complex emulsions via tunable interfacial tensions. *Nature* **518**(7540): 520–524 (2015)

[61] Sugiura S, Nakajima M, Iwamoto S, Seki M. Interfacial tension driven monodispersed droplet formation from microfabricated channel array. *Langmuir* **17**(18): 5562–5566 (2001)

[62] Sullivan D E. Surface tension and contact angle of a liquid–solid interface. *J Chem Phys* **74**(4): 2604–2615 (1981)

[63] Young T III. An essay on the cohesion of fluids. *Philos T R Soc* **95**: 65–87 (1805)

[64] Wenzel R N. Resistance of solid surfaces to wetting by water. *Ind Eng Chem* **28**(8): 988–994 (1936)

[65] Cassie A B D. Contact angles. *Discuss Faraday Soc* **3**: 11–16 (1948)

[66] Cassie A B D, Baxter S. Wettability of porous surfaces. *Trans Faraday Soc* **40**: 546–551 (1944)

[67] Grzybowski B A, Fialkowski M, Wiles J A. Kinetics of contact electrification between metals and polymers. *J Phys Chem B* **109**(43): 20511–20515 (2005)

[68] Diaz A F, Wollmann D, Dreblow D. Contact electrification: Ion transfer to metals and polymers. *Chem Mater* **3**(6): 997–999 (1991)

[69] Baytekin H T, Patashinski A Z, Branicki M, Baytekin B, Soh S, Grzybowski B A. The mosaic of surface charge in contact electrification. *Science* **333**(6040): 308–312 (2011)

[70] Li X M, Bista P, Stetten A Z, Bonart H, Schür M T, Hardt S, Bodziony F, Marschall H, Saal A, Deng X, et al. Spontaneous charging affects the motion of sliding drops. *Nat Phys* **18**(6): 713–719 (2022)

[71] Joly L, Ybert C, Trizac E, Bocquet L. Liquid friction on charged surfaces: From hydrodynamic slippage to electrokinetics. *J Chem Phys* **125**(20): 204716 (2006)

[72] Lowell J, Rose-Innes A C. Contact electrification. *Adv Phys* **29**(6): 947–1023 (1980)

[73] Xu W H, Song Y X, Xu R X, Wang Z K. Electrohydrodynamic and hydroelectric effects at the water–solid interface: From fundamentals to applications. *Adv Mater Interfaces* **8**(2): 2000670 (2021)

[74] Budakian R, Weninger K, Hiller R A, Putterman S J. Picosecond discharges and stick–slip friction at a moving meniscus of mercury on glass. *Nature* **391**(6664): 266–268 (1998)

[75] Nauruzbayeva J, Sun Z H, Gallo A Jr, Ibrahim M, Santamarina J C, Mishra H. Electrification at water–hydrophobe interfaces. *Nat Commun* **11**(1): 5285 (2020)

[76] Israelachvili J N. *Intermolecular and Surface Forces*, 3rd edn. New York (USA): Academic Press, 2011.

[77] Ise N, Yoshida H. Paradoxes of the repulsion-only assumption. *Acc Chem Res* **29**(1): 3–5 (1996)

[78] Dussan V E B. On the spreading of liquids on solid surfaces: Static and dynamic contact lines. *Annu Rev Fluid Mech* **11**: 371–400 (1979)

[79] Barrio-Zhang H, Ruiz-Gutiérrez É, Armstrong S, McHale G, Wells G G, Ledesma-Aguilar R. Contact-angle hysteresis and contact-line friction on slippery liquid-like surfaces. *Langmuir* **36**(49): 15094–15101 (2020)

[80] Wang F C, Wu H A. Pinning and depinning mechanism of the contact line during evaporation of nano-droplets sessile on textured surfaces. *Soft Matter* **9**(24): 5703 (2013)

[81] Chen Z, Khajeh A, Martini A, Kim S H. Chemical and physical origins of friction on surfaces with atomic steps. *Sci Adv* **5**(8): eaaw0513 (2019)

[82] Raviv U, Klein J. Fluidity of bound hydration layers. *Science* **297**(5586): 1540–1543 (2002)

[83] Choi K S, Yang X, Clayton B R, Glover E J, Atlar M, Semenov B N, Kulik V M. Turbulent drag reduction using compliant surfaces. *P Roy Soc A-Math Phy* **453**(1965): 2229–2240 (1997)

[84] Tcholakova S, Denkov N D, Golemanov K, Ananthapadmanabhan K P, Lips A. Theoretical model of viscous friction inside steadily sheared foams and concentrated emulsions. *Phys Rev E* **78**(1): 011405 (2008)

[85] Erbaş A, Horinek D, Netz R R. Viscous friction of hydrogen-bonded matter. *J Am Chem Soc* **134**(1): 623–630 (2012)

[86] Bosanquet C H. LV. On the flow of liquids into capillary tubes. *Lond Edinb Dublin Philos Mag J Sci* **45**(267): 525–531 (1923)

[87] Radin I, Zakin J L, Patterson G K. Drag reduction of solid–liquid suspensions in pipe flow. *Nat Phys Sci* **246**(149): 11–13 (1973)

[88] Liu M, Ma L R. Drag reduction methods at solid–liquid interfaces. *Friction* **10**(4): 491–515 (2022)

[89] Wenzel R N. Surface roughness and contact angle. *J Phys Chem* **53**(9): 1466–1467 (1949)

[90] Extrand C W. Contact angles and hysteresis on surfaces with chemically heterogeneous islands. *Langmuir* **19**(9): 3793–3796 (2003)

[91] Gao L C, McCarthy T J. How Wenzel and Cassie were wrong. *Langmuir* **23**(7): 3762–3765 (2007)

[92] Snoeijer J H, Andreotti B. Moving contact lines: Scales, regimes, and dynamical transitions. *Annu Rev Fluid Mech* **45**: 269–292 (2013)

[93] Bonn D, Eggers J, Indekeu J, Meunier J, Rolley E. Wetting and spreading. *Rev Mod Phys* **81**(2): 739–805 (2009)

[94] Ramiasa M, Ralston J, Fetzer R, Sedev R. Contact line friction in liquid–liquid displacement on hydrophobic surfaces. *J Phys Chem C* **115**(50): 24975–24986 (2011)

[95] Wong T S, Kang S H, Tang S K, Smythe E J, Hatton B D, Grinthal A, Aizenberg J. Bioinspired self-repairing slippery surfaces with pressure-stable omniphobicity. *Nature* **477**(7365): 443–447 (2011)

[96] Rong W T, Zhang H F, Zhang T J, Mao Z G, Liu X W, Song K G. Drag reduction using lubricant-impregnated anisotropic slippery surfaces inspired by bionic fish scale surfaces containing micro-/ nanostructured arrays. *Adv Eng Mater* **23**(1): 2000821 (2021)

[97] Wang L M, McCarthy T J. Covalently attached liquids: Instant omniphobic surfaces with unprecedented repellency. *Angew Chem Int Ed* **55**(1): 244–248 (2016)

[98] Armstrong S, McHale G, Ledesma-Aguilar R, Wells G G. Pinning-free evaporation of sessile droplets of water from solid surfaces. *Langmuir* **35**(8): 2989–2996 (2019)

[99] Johansson P, Hess B. Molecular origin of contact line friction in dynamic wetting. *Phys Rev Fluids* **3**(7): 074201 (2018)

[100] Pendry J B. Quantum friction—Fact or fiction? *New J Phys* **12**(3): 033028 (2010)

[101] Marino J, Recati A, Carusotto I. Casimir forces and quantum friction from Ginzburg radiation in atomic Bose-Einstein condensates. *Phys Rev Lett* **118**(4): 045301 (2017)

[102] Volokitin A I, Persson B N J. Quantum friction. *Phys Rev Lett* **106**(9): 094502 (2011)

[103] Zhang X, Huang Y L, Ma Z S, Niu L Y, Sun C Q. From ice superlubricity to quantum friction: Electronic repulsivity and phononic elasticity. *Friction* **3**(4): 294–319 (2015)

[104] De Bièvre S, Faupin J, Schubnel B. Spectral analysis of a model for quantum friction. *Rev Math Phys* **29**(6): 1750019 (2017)

[105] Deng S J, Chenu A, Diao P P, Li F, Yu S, Coulamy I, del Campo A, Wu H B. Superadiabatic quantum friction

suppression in finite-time thermodynamics. *Sci Adv* **4**(4): eaar5909 (2018)

[106] Howell H G. The laws of friction. *Nature* **171**(4344): 220 (1953)

[107] Stipe B C, Mamin H J, Stowe T D, Kenny T W, Rugar D. Noncontact friction and force fluctuations between closely spaced bodies. *Phys Rev Lett* **87**(9): 096801 (2001)

[108] Kuehn S, Loring R F, Marohn J A. Dielectric fluctuations and the origins of noncontact friction. *Phys Rev Lett* **96**(15): 156103 (2006)

[109] Volokitin A I, Persson B N J. Near-field radiative heat transfer and noncontact friction. *Rev Mod Phys* **79**(4): 1291–1329 (2007)

[110] She J H, Balatsky A V. Noncontact friction and relaxational dynamics of surface defects. *Phys Rev Lett* **108**(13): 136101 (2012)

[111] Lee M, Kim B, Kim J, Jhe W. Noncontact friction via capillary shear interaction at nanoscale. *Nat Commun* **6**: 7359 (2015)

[112] Lee M R, Vink R L C, Volkert C A, Krüger M. Noncontact friction: Role of phonon damping and its nonuniversality. *Phys Rev B* **104**(17): 174309 (2021)

[113] Navier C L. Sur les lois de l'équilibre et du mouvement des corps élastiques. *Mem Acad R Sci Inst France* **6**: 369 (1827) (in French)

[114] Stokes G G. On the effect of the internal friction of fluids on the motion of pendulums. *Proc Cambridge Philos Soc* **9**: 8 (1850)

[115] Phan, D T T, Wang X L, Craver B M, Sobrino, A, Zhao D, Chen C J, Lee L Y N, Gorge, S C, Lee A P, Hughes, C C W. A vascularized and perfused organ-on-a-chip platform for large-scale drug screening applications. *Lab Chip* **17**(3): 511–520 (2017)

[116] Bocquet L, Charlaix E. Nanofluidics, from bulk to interfaces. *Chem Soc Rev* **39**(3): 1073–1095 (2010)

[117] Neto C, Evans D R, Bonaccurso E, Butt H J, Craig V S J. Boundary slip in Newtonian liquids: A review of experimental studies. *Rep Prog Phys* **68**(12): 2859–2897 (2005)

[118] Bocquet L, Barrat J L. Flow boundary conditions from nano- to micro-scales. *Soft Matter* **3**(6): 685–693 (2007)

[119] Chen S Y, Doolen G D. Lattice Boltzmann method for fluid flows. *Annu Rev Fluid Mech* **30**: 329–364 (1998)

[120] McNamara G R, Zanetti G. Use of the Boltzmann equation to simulate lattice gas automata. *Phys Rev Lett* **61**(20): 2332–2335 (1988)

[121] Taher M A, Kim H D, Lee Y W. LBM simulation on friction and mass flow analysis in a rough microchannel. *J Korean Soc Mar Eng* **38**(10): 1237–1243 (2014)

[122] Huang J J, Shu C, Chew Y T. Lattice Boltzmann study of droplet motion inside a grooved channel. *Phys Fluids* **21**(2): 022103 (2009)

[123] Dubov A L, Schmieschek S, Asmolov E S, Harting J, Vinogradova O I. Lattice-Boltzmann simulations of the drag force on a sphere approaching a superhydrophobic striped plane. *J Chem Phys* **140**(3): 034707 (2014)

[124] Tomlinson G A. CVI. A molecular theory of friction. *Lond Edinb Dublin Philos Mag J Sci* **7**(46): 905–939 (1929)

[125] Bowden, F P, Tabor, D. The area of contact between stationary and moving surfaces. *Proceedings of the Royal Society of London. Series A. Mathematical and Physical Sciences* **169**(938): 391–413 (1938).

[126] Metropolis N, Rosenbluth A W, Rosenbluth M N, Teller A H, Teller E. Equation of state calculations by fast computing machines. *J Chem Phys* **21**(6): 1087–1092 (1953)

[127] Balasubramanian S, Mundy C J. Calculation of friction coefficient of a solid–liquid interface via a non-equilibrium molecular dynamics simulation. *B Mater Sci* **22**(5): 873–876 (1999)

[128] Petravic J, Harrowell P. On the equilibrium calculation of the friction coefficient for liquid slip against a wall. *J Chem Phys* **127**(17): 174706 (2007)

[129] Tocci G, Joly L, Michaelides A. Friction of water on graphene and hexagonal boron nitride from *ab initio* methods: Very different slippage despite very similar interface structures. *Nano Lett* **14**(12): 6872–6877 (2014)

[130] Falk K, Sedlmeier F, Joly L, Netz R R, Bocquet L. Molecular origin of fast water transport in carbon nanotube membranes: Superlubricity versus curvature dependent friction. *Nano Lett* **10**(10): 4067–4073 (2010)

[131] Thomas J A, McGaughey A J H. Reassessing fast water transport through carbon nanotubes. *Nano Lett* **8**(9): 2788–2793 (2008)

[132] Bocquet L, Barrat J L. Hydrodynamic boundary conditions, correlation functions, and Kubo relations for confined fluids. *Phys Rev E* **49**(4): 3079–3092 (1994)

[133] Bocquet L, Barrat J. Hydrodynamic boundary conditions and correlation functions of confined fluids. *Phys Rev Lett* **70**(18): 2726–2729 (1993)

[134] Huang K, Szlufarska I. Green–Kubo relation for friction at liquid–solid interfaces. *Phys Rev E* **89**(3): 032119 (2014)

[135] Bocquet L, Barrat J L. On the Green–Kubo relationship for the liquid–solid friction coefficient. *J Chem Phys* **139**(4): 044704 (2013)

[136] Oga H, Yamaguchi Y, Omori T, Merabia S, Joly L. Green–Kubo measurement of liquid–solid friction in finite-size systems. *J Chem Phys* **151**(5): 054502 (2019)

[137] Wu Y, Wei Q B, Cai M R, Zhou F. Interfacial friction control. *Adv Mater Interfaces* **2**(2): 1400392 (2015)

[138] Wang Z B, Xu Q, Wang L L, Heng L P, Jiang L. Temperature-induced switchable interfacial interactions on slippery surfaces for controllable liquid manipulation. *J Mater Chem A* **7**(31): 18510–18518 (2019)

[139] Zheng F, Lv M, Wang Q H, Wang T M. Effect of temperature on friction and wear behaviors of polyimide (PI)-based solid–liquid lubricating materials. *Polym Advan Technol* **26**(8): 988–993 (2015)

[140] McGhee E O, Urueña J M, Pitenis A A, Sawyer W G. Temperature-dependent friction of gemini hydrogels. *Tribol Lett* **67**(4): 117 (2019)

[141] Hu N N, Wu N, Wang S Q, Jiang H B, Li Z P. Tribological properties of friction pairs in lubricant contaminated with particles under high temperature. *Tribol Trans* **60**(4): 663–669 (2017)

[142] Persson B N J. Ice friction: Glacier sliding on hard randomly rough bed surface. *J Chem Phys* **149**(23): 234701 (2018)

[143] Ewen J P, Gao H Y, Müser M H, Dini D. Shear heating, flow, and friction of confined molecular fluids at high pressure. *Phys Chem Chem Phys* **21**(10): 5813–5823 (2019)

[144] Wang Y N, Zhang Y F, Tang C, Yu J X, He H T, Qi H M. Solid/liquid interfacial friction and slip behaviors on roughness surface under applied voltage. *Tribol Int* **144**: 106128 (2020)

[145] Zhang Y F, Wang Y N, Wu X L, Tang C, Liu Z H, Zhou G Y, Yu J X. Combined effects of pinning and adhesion force on solid/liquid interfacial friction behaviors under applied voltage. *Tribol Int* **134**: 102–108 (2019)

[146] Morooka T, Sagara T. Electrowetting of hydrofluoroether liquid droplet at a gold electrode/water interface: Significance of lower adhesion energy and static friction energy. *Langmuir* **36**(33): 9685–9692 (2020)

[147] Acharya B, Seed C M, Brenner D W, Smirnov A I, Krim J. Tuning friction and slip at solid-nanoparticle suspension interfaces by electric fields. *Sci Rep* **9**: 18584 (2019)

[148] Jin Y K, Xu W H, Zhang H H, Li R R, Sun J, Yang S Y, Liu M J, Mao H Y, Wang Z K. Electrostatic tweezer for droplet manipulation. *PNAS* **119**(2): e2105459119 (2022)

[149] Wu Y, Liu Z L, Liang Y M, Pei X W, Zhou F, Xue Q J. Photoresponsive superhydrophobic coating for regulating boundary slippage. *Soft Matter* **10**(29): 5318–5324 (2014)

[150] Lai Y K, Huang J Y, Cui Z Q, Ge M Z, Zhang K Q, Chen Z, Chi L F. Recent advances in TiO_2-based nanostructured surfaces with controllable wettability and adhesion. *Small* **12**(16): 2203–2224 (2016)

[151] Ben S, Zhou T T, Ma H, Yao J J, Ning Y Z, Tian D L, Liu K S, Jiang L. Multifunctional magnetocontrollable superwettable-microcilia surface for directional droplet manipulation. *Adv Sci* **6**(17): 1900834 (2019)

[152] Huang K, Szlufarska I. Friction and slip at the solid/liquid interface in vibrational systems. *Langmuir* **28**(50): 17302–17312 (2012)

[153] Genzer J, Efimenko K. Creating long-lived superhydrophobic polymer surfaces through mechanically assembled monolayers. *Science* **290**(5499): 2130–2133 (2000)

[154] Hao C L, Li J, Liu Y, Zhou X F, Liu Y H, Liu R, Che L F, Zhou W Z, Sun D, Li L, et al. Superhydrophobic-like tunable droplet bouncing on slippery liquid interfaces. *Nat Commun* **6**: 7986 (2015)

[155] Bohn H F, Federle W. Insect aquaplaning: *Nepenthes* pitcher plants capture prey with the peristome, a fully wettable water-lubricated anisotropic surface. *PNAS* **101**(39): 14138–14143 (2004)

[156] Jin Z M, Dowson D. Bio-friction. *Friction* **1**(2): 100–113 (2013)

[157] Greene G W, Banquy X, Lee D W, Lowrey D D, Yu J, Israelachvili J N. Adaptive mechanically controlled lubrication mechanism found in articular joints. *PNAS* **108**(13): 5255–5259 (2011)

[158] Neville A, Morina A, Liskiewicz T, Yan Y. Synovial joint lubrication—Does nature teach more effective engineering lubrication strategies? *P I Mech Eng C-J Mech Eng Sci* **221**(10): 1223–1230 (2007)

[159] Dintenfass L. Lubrication in synovial joints. *Nature* **197**(4866): 496–497 (1963)

[160] Mouza A, Skordia O, Tzouganatos I, Paras S. A simplified model for predicting friction factors of laminar blood flow in small-caliber vessels. *Fluids* **3**(4): 75 (2018)

[161] Huang X Z, Wu J, Zhu Y D, Zhang Y M, Feng X, Lu X H. Flow-resistance analysis of nano-confined fluids inspired from liquid nano-lubrication: A review. *Chin J Chem Eng* **25**(11): 1552–1562 (2017)

[162] Sweeney J, Hausen F, Hayes R, Webber G B, Endres F, Rutland M W, Bennewitz R, Atkin R. Control of nanoscale friction on gold in an ionic liquid by a potential-dependent ionic lubricant layer. *Phys Rev Lett* **109**(15): 155502 (2012)

[163] Capozza R, Benassi A, Vanossi A, Tosatti E. Electrical charging effects on the sliding friction of a model nano-confined ionic liquid. *J Chem Phys* **143**(14): 144703 (2015)

[164] Sweeney J, Webber G B, Atkin R. Poly(ethylene oxide) mushrooms adsorbed at silica-ionic liquid interfaces reduce friction. *Langmuir* **32**(8): 1947–1954 (2016)

[165] Radiom M. Ionic liquid–solid interface and applications in lubrication and energy storage. *Curr Opin Colloid In* **39**: 148–161 (2019)

[166] Fajardo O Y, Bresme F, Kornyshev A A, Urbakh M. Electrotunable friction with ionic liquid lubricants: How important is the molecular structure of the ions? *J Phys Chem Lett* **6**(20): 3998–4004 (2015)

[167] Liefferink R W, Hsia F C, Weber B, Bonn D. Friction on ice: How temperature, pressure, and speed control the slipperiness of ice. *Phys Rev X* **11**(1): 011025 (2021)

[168] Kietzig A M, Hatzikiriakos S G, Englezos P. Physics of ice friction. *J Appl Phys* **107**(8): 081101 (2010)

[169] Louden P B, Gezelter J D. Friction at ice-I_h/water interfaces is governed by solid/liquid hydrogen-bonding. *J Phys Chem C* **121**(48): 26764–26776 (2017)

[170] Persson B N J. Ice friction: Role of non-uniform frictional heating and ice premelting. *J Chem Phys* **143**(22): 224701 (2015)

[171] Kietzig A M, Hatzikiriakos S G, Englezos P. Ice friction: The effects of surface roughness, structure, and hydrophobicity. *J Appl Phys* **106**(2): 024303 (2009)

[172] Verberck B. Slippy nitty-gritty. *Nat Phys* **17**(3): 302 (2021)

[173] Louden P B, Gezelter J D. Simulations of solid–liquid friction at ice-I_h/water interfaces. *J Chem Phys* **139**(19): 194710 (2013)

[174] Dash J G. Surface melting. *Contemp Phys* **30**(2): 89–100 (1989)

[175] Macconaill M A. Lubrication of mammalian joints. *Nature* **185**(4717): 920 (1960)

[176] Ruggiero A. Milestones in natural lubrication of synovial joints. *Front Mech Eng* **6**: 52 (2020)

[177] Suhardi V J, Bichara D A, Kwok S, Freiberg A A, Rubash H, Malchau H, Yun S H, Muratoglu O K, Oral E. A fully functional drug-eluting joint implant. *Nat Biomed Eng* **1**: 0080 (2017)

[178] Zhang Y L, Zhao W Y, Ma S H, Liu H, Wang X W, Zhao X D, Yu B, Cai M R, Zhou F. Modulus adaptive lubricating prototype inspired by instant muscle hardening mechanism of catfish skin. *Nat Commun* **13**(1): 377 (2022)

[179] Chester F M, Rowe C, Ujiie K, Kirkpatrick J, Regalla C, Remitti F, Moore J C, Toy V, Wolfson-Schwehr M, Bose S, et al. Structure and composition of the plate-boundary slip zone for the 2011 Tohoku-Oki earthquake. *Science* **342**(6163): 1208–1211 (2013)

[180] Sutherland R, Townend J, Toy V, Upton P, Coussens J, Allen M, Baratin L M, Barth N, Becroft L, Boese C, et al. Extreme hydrothermal conditions at an active plate-bounding fault. *Nature* **546**(7656): 137–140 (2017)

[181] Li J Q, Zheng H X, Yang Z B, Wang Z K. Breakdown in the directional transport of droplets on the peristome of pitcher plants. *Commun Phys* **1**: 35 (2018)

[182] Chen H W, Zhang P F, Zhang L W, Liu H L, Jiang Y, Zhang D Y, Han Z W, Jiang L. Continuous directional water transport on the peristome surface of *Nepenthes alata*. *Nature* **532**(7597): 85–89 (2016)

[183] Li J Q, Song Y X, Zheng H X, Feng S L, Xu W H, Wang Z K. Designing biomimetic liquid diodes. *Soft Matter* **15**(9): 1902–1915 (2019)

[184] Li J, Li J Q, Sun J, Feng S L, Wang Z K. Biological and engineered topological droplet rectifiers. *Adv Mater* **31**(14): 1806501 (2019)

[185] Wang C L, Lu H J, Wang Z G, Xiu P, Zhou B, Zuo G H, Wan R Z, Hu J, Fang H P. Stable liquid water droplet on a water monolayer formed at room temperature on ionic model substrates. *Phys Rev Lett* **103**(13): 137801 (2009)

[186] Lee K, Kim Q, An S, An J, Kim J, Kim B, Jhe W. Superwetting of TiO_2 by light-induced water-layer growth via delocalized surface electrons. *PNAS* **111**(16): 5784–5789 (2014)

[187] Wang C L, Wen B H, Tu Y S, Wan R Z, Fang H P. Friction reduction at a superhydrophilic surface: Role of ordered water. *J Phys Chem C* **119**(21): 11679–11684 (2015)

[188] Zhong X W, Xia Y Q, Feng X. Tribological application and mechanism of epicuticular wax. *Friction* **7**(1): 44–58 (2019)

[189] Xia Y Q, Xu X C, Feng X, Chen G X. Leaf-surface wax of desert plants as a potential lubricant additive. *Friction* **3**(3): 208–213 (2015)

[190] Ren Y L, Zhang L, Xie G X, Li Z B, Chen H, Gong H J, Xu W H, Guo D, Luo J B. A review on tribology of polymer composite coatings. *Friction* **9**(3): 429–470 (2021)

[191] Liu J J, Qu S X, Suo Z G, Yang W. Functional hydrogel coatings. *Natl Sci Rev* **8**(2): nwaa254 (2021)

[192] McHale G, Newton M I. Liquid marbles: Principles and applications. *Soft Matter* **7**(12): 5473–5481 (2011)

[193] Kasahara M, Akimoto S I, Hariyama T, Takaku Y, Yusa S I, Okada S, Nakajima K, Hirai T, Mayama H, Okada S, et al. Liquid marbles in nature: Craft of aphids for survival. *Langmuir* **35**(18): 6169–6178 (2019)

[194] Aussillous P, Quéré D. Liquid marbles. *Nature* **411**(6840): 924–927 (2001)

[195] Aussillous P, Quéré D. Properties of liquid marbles. *P Roy Soc A-Math Phy* **462**(2067): 973–999 (2006)

[196] Sarvi F, Jain K, Arbatan T, Verma P J, Hourigan K, Thompson M C, Shen W, Chan P P. Cardiogenesis of embryonic stem cells with liquid marble micro-bioreactor. *Adv Healthc Mater* **4**(1): 77–86 (2015)

[197] Ooi C H, van Nguyen A, Evans G M, Dao D V, Nguyen N T. Measuring the coefficient of friction of a small floating liquid marble. *Sci Rep* **6**: 38346 (2016)

[198] Leidenfrost J G. *De Aquae Communis Nonnullis Qualitatibus Tractatus*. City (Country): Ovenius, 1756. (in language)

[199] Li J, Hou Y M, Liu Y H, Hao C L, Li M F, Chaudhury M K, Yao S H, Wang Z K. Directional transport of high-temperature Janus droplets mediated by structural topography. *Nat Phys* **12**(6): 606–612 (2016)

[200] Zhang P P, Peng B X, Wang J M, Jiang L. Bioinspired self-propulsion of water droplets at the convergence of Janus-textured heated substrates. *Adv Funct Mater* **29**(39): 1904535 (2019)

[201] Dodd L E, Wood D, Geraldi N R, Wells G G, McHale G, Xu B B, Stuart-Cole S, Martin J, Newton M I. Low friction droplet transportation on a substrate with a selective Leidenfrost effect. *ACS Appl Mater Inter* **8**(34): 22658–22663 (2016)

[202] Dodd L E, Agrawal P, Parnell M T, Geraldi N R, Xu B B, Wells G G, Stuart-Cole S, Newton M I, McHale G, Wood D. Low-friction self-centering droplet propulsion and transport using a Leidenfrost herringbone–ratchet structure. *Phys Rev Appl* **11**(3): 034063 (2019)

[203] Lagubeau G, Le Merrer M, Clanet C, Quéré D. Leidenfrost on a ratchet. *Nat Phys* **7**(5): 395–398 (2011)

[204] Truesdell R, Mammoli A, Vorobieff P, van Swol F, Brinker C J. Drag reduction on a patterned superhydrophobic surface. *Phys Rev Lett* **97**(4): 044504 (2006)

[205] Ybert C, Barentin C, Cottin-Bizonne C, Joseph P, Bocquet L. Achieving large slip with superhydrophobic surfaces: Scaling laws for generic geometries. *Phys Fluids* **19**(12): 123601 (2007)

[206] Zhao L, Cheng J T. The mechanism and universal scaling law of the contact line friction for the Cassie-state droplets on nanostructured ultrahydrophobic surfaces. *Nanoscale* **10**(14): 6426–6436 (2018)

[207] Wu Y, Cai M R, Li Z Q, Song X W, Wang H Y, Pei X W, Zhou F. Slip flow of diverse liquids on robust superomniphobic surfaces. *J Colloid Interf Sci* **414**: 9–13 (2014)

[208] Rothstein J P. Slip on superhydrophobic surfaces. *Annu Rev Fluid Mech* **42**: 89–109 (2010)

[209] Ceccio S L. Friction drag reduction of external flows with bubble and gas injection. *Annu Rev Fluid Mech* **42**: 183–203 (2010)

[210] Steinberger A, Cottin-Bizonne C, Kleimann P, Charlaix E. High friction on a bubble mattress. *Nat Mater* **6**(9): 665–668 (2007)

[211] Lu J C, Fernández A, Tryggvason G. The effect of bubbles on the wall drag in a turbulent channel flow. *Phys Fluids* **17**(9): 095102 (2005)

[212] Hyväluoma J, Harting J. Slip flow over structured surfaces with entrapped microbubbles. *Phys Rev Lett* **100**(24): 246001 (2008)

[213] Finger A, Johannsmann D. Hemispherical nanobubbles reduce interfacial slippage in simple liquids. *Phys Chem Chem Phys* **13**(40): 18015–18022 (2011)

[214] Park H, Choi C H, Kim C J. Superhydrophobic drag reduction in turbulent flows: A critical review. *Exp Fluids* **62**(11): 229 (2021)

[215] Barthlott W, Neinhuis C. Purity of the sacred lotus, or escape from contamination in biological surfaces. *Planta* **202**(1): 1–8 (1997)

[216] Barthlott W. Die Selbstreinigungsfähigkeit pflanzlicher Oberflächen durch Epicuticularwachse. In: *Verantwortung für Die Zukunft*. Klima-und Umweltforschung an der Universität Bonn, 1992: 117–120. (in Germany)

[217] Mertaniemi H, Jokinen V, Sainiemi L, Franssila S, Marmur A, Ikkala O, Ras R H. Superhydrophobic tracks for low-friction, guided transport of water droplets. *Adv Mater* **23**(26): 2911–2914 (2011)

[218] Liu Y H, Wang Z K. Superhydrophobic porous networks for enhanced droplet shedding. *Sci Rep* **6**: 33817 (2016)

[219] Hao C L, Zhou Y, Zhou X F, Che L F, Chu B J, Wang Z K. Dynamic control of droplet jumping by tailoring nanoparticle concentrations. *Appl Phys Lett* **109**(2): 021601 (2016)

[220] Choi C H, Kim C J. Large slip of aqueous liquid flow over a nanoengineered superhydrophobic surface. *Phys Rev Lett* **96**(6): 066001 (2006)

[221] Li F D, Hou H H, Yin J, Jiang X S. Near-infrared light-responsive dynamic wrinkle patterns. *Sci Adv* **4**(4): eaar5762 (2018)

[222] Erbil H Y, Demirel A L, Avcı Y, Mert O. Transformation of a simple plastic into a superhydrophobic surface. *Science* **299**(5611): 1377–1380 (2003)

[223] Li X M, Yang J L, Lv K X, Papadopoulos P, Sun J, Wang D H, Zhao Y H, Chen L Q, Wang D P, Wang Z K, et al. *Salvinia*-like slippery surface with stable and mobile water/air contact line. *Natl Sci Rev* **8**(5): nwaa153 (2021)

[224] Yun G T, Jung W B, Oh M S, Jang G M, Baek J, Kim N I, Im S G, Jung H T. Springtail-inspired superomniphobic surface with extreme pressure resistance. *Sci Adv* **4**(8): eaat4978 (2018)

[225] Sun J, Zhu P G, Yan X T, Zhang C, Jin Y K, Chen X, Wang Z K. Robust liquid repellency by stepwise wetting resistance. *Appl Phys Rev* **8**(3): 031403 (2021)

[226] Savchenko Y N. Supercavitation—Problems and perspectives. In: Proceedings of the CAV 2001: Fourth International Symposium on Cavitation, Pasadena, USA, 2001: CAV2001:lecture.003.

[227] Serebryakov V V. Supercavitation for high speed motion in water: Prediction and drag reduction problems. In: Proceedings of the ASME 2002 Joint U.S.–European Fluids Engineering Division Conference, Montreal, Canada, 2002: 411–417.

[228] Patek S N, Caldwell R L. Extreme impact and cavitation forces of a biological hammer: Strike forces of the peacock mantis shrimp *Odontodactylus scyllarus*. *J Exp Biol* **208**(19): 3655–3664 (2005)

[229] Zia H, Lecampion B. Propagation of a height contained hydraulic fracture in turbulent flow regimes. *Int J Solids Struct* **110–111**: 265–278 (2017)

[230] Nikuradse J. *Laws of Flow in Rough Pipes*. Washington (USA): NACA, 1950.

[231] Yang S Q, Dou G. Turbulent drag reduction with polymer additive in rough pipes. *J Fluid Mech* **642**: 279–294 (2010)

[232] Virk P S. Drag reduction in rough pipes. *J Fluid Mech* **45**(2): 225–246 (1971)

[233] Xu B, Ooti K T, Wong N T, Choi W K. Experimental investigation of flow friction for liquid flow in microchannels. *Int Commun Heat Mass* **27**(8): 1165–1176 (2000)

[234] Lv M, Yang L J, Wang Q H, Wang T M, Liang Y M. Tribological performance and lubrication mechanism of solid–liquid lubricating materials in high-vacuum and irradiation environments. *Tribol Lett* **59**(1): 20 (2015)

[235] Quere D. Leidenfrost dynamics. *Annu Rev Fluid Mech* **45**: 197–215

[236] Berim G O, Ruckenstein E. Dependence of the macroscopic contact angle on the liquid–solid interaction parameters and temperature. *J Chem Phys* **130**(18): 184712 (2009)

[237] Berim G O, Ruckenstein E. Simple expression for the dependence of the nanodrop contact angle on liquid–solid interactions and temperature. *J Chem Phys* **130**(4): 044709 (2009)

[238] Wu Y, Xue Y H, Pei X W, Cai M R, Duan H L, Huck W T S, Zhou F, Xue Q J. Adhesion-regulated switchable fluid slippage on superhydrophobic surfaces. *J Phys Chem C* **118**(5): 2564–2569 (2014)

[239] Jing D L, Bhushan B. The coupling of surface charge and boundary slip at the solid–liquid interface and their combined effect on fluid drag: A review. *J Colloid Interf Sci* **454**: 152–179 (2015)

[240] Li X M, Tian H M, Shao J Y, Ding Y C, Chen X L, Wang L, Lu B H. Decreasing the saturated contact angle in electrowetting-on-dielectrics by controlling the charge trapping at liquid–solid Interfaces. *Adv Funct Mater* **26**(18): 2994–3002 (2016)

[241] Shahzad A, Wijewardhana K R, Song J K. Contact electrification efficiency dependence on surface energy at the water–solid interface. *Appl Phys Lett* **113**(2): 023901 (2018)

[242] Sun Q Q, Wang D H, Li Y N, Zhang J H, Ye S J, Cui J X, Chen L Q, Wang Z K, Butt H J, Vollmer D, et al. Surface charge printing for programmed droplet transport. *Nat Mater* **18**(9): 936–941 (2019)

[243] Bechert D W, Bruse M, Hage W. Experiments with three-dimensional riblets as an idealized model of shark skin. *Exp Fluids* **28**(5): 403–412 (2000)

[244] Dean B, Bhushan B. Shark-skin surfaces for fluid-drag reduction in turbulent flow: A review. *Philos Trans A Math Phys Eng Sci* **368**(1929): 4775–4806 (2010)

[245] Wen L, Weaver J C, Lauder G V. Biomimetic shark skin: Design, fabrication and hydrodynamic function. *J Exp Biol* **217**(Pt 10): 1656–1666 (2014)

[246] Tenan M A, Hackwood S, Beni G. Friction in capillary systems. *J Appl Phys* **53**(10): 6687–6692 (1982)

[247] Tenjimbayashi M, Kawamura K, Shiratori S. Continuous directional water transport on hydrophobic slippery ventral skin of *Lampropeltis pyromelana*. *Adv Mater Interfaces* **7**(19): 2000984 (2020)

[248] Chaudhury M K, Whitesides G M. How to make water run uphill. *Science* **256**(5063): 1539–1541 (1992)

[249] Liu C R, Sun J, Li J, Xiang C H, Che L F, Wang Z K, Zhou X F. Long-range spontaneous droplet self-propulsion on wettability gradient surfaces. *Sci Rep* **7**: 7552 (2017)

[250] Chu K H, Xiao R, Wang E N. Uni-directional liquid spreading on asymmetric nanostructured surfaces. *Nat Mater* **9**(5): 413–417 (2010)

[251] Chen H W, Zhang L W, Zhang P F, Zhang D Y, Han Z W, Jiang L. A novel bioinspired continuous unidirectional liquid spreading surface structure from the peristome surface of *Nepenthes* alata. *Small* **13**(4): 1601676 (2017)

[252] Li J, Zhou X, Li J, Che L, Yao J, McHale G, Chaudhury MK, Wang Z. Topological liquid diode. *Sci Adv* **3**(10): eaao3530 (2017)

[253] Sun W X, Tang L J, Hong W, Zhan Y J, Yang B, Liu J Q. A novel microstructure inspired from *Nepenthes* alata and lizard skin and its enhanced uni-directional liquid spreading property. *RSC Adv* **9**(14): 7842–7848 (2019)

[254] Hou X H, Yu J K, Sheng M K, Yang X. Influencing factors to the friction charging in water delivery metal pipeline. *J Electrostat* **82**: 7–10 (2016)

[255] Larsson L, Raven H C, Pauling J R. *The Principles of Naval Architecture Series: Ship Resistance and Flow*. Jersey

City (USA): The Society of Naval Architects and Marine Engineers, 2010.

[256] Luhar M. Turbulence Control—Peace in the pipeline. *Nat Phys* **14**(4): 336–337 (2018)

[257] Suzuki K, Taketomi T, Sato S. Improving Zielke's method of simulating frequency-dependent friction in laminar liquid pipe flow. *J Fluids Eng* **113**(4): 569–573 (1991)

[258] Kurakina M Y, Radchenko V P, Yufin V A. Nonsteady motion of a dropping compressible liquid in pipes under different laws of friction. *J Appl Mech Tech Phys* **17**(1): 69–74 (1976)

[259] Kühnen J, Song B F, Scarselli D, Budanur N B, Riedl M, Willis A P, Avila M, Hof B. Destabilizing turbulence in pipe flow. *Nat Phys* **14**(4): 386–390 (2018)

[260] Trikha A K. An efficient method for simulating frequency-dependent friction in transient liquid flow. *J Fluids Eng* **97**(1): 97–105 (1975)

[261] Vilquin A, Jagielka J, Djambov S, Herouard H, Fisher P, Bruneau C H, Chakraborty P, Gioia G, Kellay H. Asymptotic turbulent friction in 2D rough-walled flows. *Sci Adv* **7**(5): eabc6234 (2021)

[262] Pucci G, Ho I, Harris D M. Friction on water sliders. *Sci Rep* **9**: 4095 (2019)

[263] Shugai A A. Friction of solid bodies with formation of a melt layer. *J Eng Phys Thermophys* **72**(5): 963–971 (1999)

[264] Yang C Y. Friction characteristics of water, R-134a, and air in small tubes. *Microsc Therm Eng* **7**(4): 335–348 (2003)

[265] Steinke M E, Kandlikar S G. Single-phase liquid friction factors in microchannels. *Int J Therm Sci* **45**(11): 1073–1083 (2006)

[266] Cottin-Bizonne C, Barrat J L, Bocquet L, Charlaix E. Low-friction flows of liquid at nanopatterned interfaces. *Nat Mater* **2**(4): 237–240 (2003)

[267] Brutin D, Topin F, Tadrist L. Transient method for the liquid laminar flow friction factor in microtubes. *AIChE J* **49**(11): 2759–2767 (2003)

[268] Zhang P, Zuo C C, Liu X T. Study on friction coefficient of liquid flow through a rectangular microchannel with electrokinetic effects. In: Proceedings of the 2010 International Conference on Digital Manufacturing & Automation, Changcha, China, 2010: 485–489.

[269] Mouterde T, Keerthi A, Poggioli A R, Dar S A, Siria A, Geim A K, Bocquet L, Radha B. Molecular streaming and its voltage control in ångström-scale channels. *Nature* **567**(7746): 87–90 (2019)

[270] Falk K, Sedlmeier F, Joly L, Netz R R, Bocquet L. Ultralow liquid/solid friction in carbon nanotubes: Comprehensive theory for alcohols, alkanes, OMCTS, and water. *Langmuir* **28**(40): 14261–14272 (2012)

[271] Raviv U, Laurat P, Klein J. Fluidity of water confined to subnanometre films. *Nature* **413**(6851): 51–54 (2001)

[272] Hummer G, Rasaiah J C, Noworyta J P. Water conduction through the hydrophobic channel of a carbon nanotube. *Nature* **414**(6860): 188–190 (2001)

[273] Persson B N J, Tartaglino U, Tosatti E, Ueba H. Electronic friction and liquid-flow-induced voltage in nanotubes. *Phys Rev B* **69**(23): 235410 (2004)

[274] Sokoloff J B. Effects of electronic friction from the walls on water flow in carbon nanotubes and on water desalination. *Phys Rev E* **100**(2): 023112 (2019)

[275] Sokoloff J B. Enhancement of the water flow velocity through carbon nanotubes resulting from the radius dependence of the friction due to electron excitations. *Phys Rev E* **97**(3): 033107 (2018)

[276] Oyarzua E, Walther J H, Zambrano H A. Water thermophoresis in carbon nanotubes: The interplay between thermophoretic and friction forces. *Phys Chem Chem Phys* **20**(5): 3672–3677 (2018)

[277] Ma M, Grey F, Shen L M, Urbakh M, Wu S, Liu J Z, Liu Y L, Zheng Q S. Water transport inside carbon nanotubes mediated by phonon-induced oscillating friction. *Nat Nanotechnol* **10**(8): 692–695 (2015)

[278] Babu J S, Sathian S P. Combining molecular dynamics simulation and transition state theory to evaluate solid–liquid interfacial friction in carbon nanotube membranes. *Phys Rev E* **85**(5): 051205 (2012)

[279] Ou J, Perot B, Rothstein J P. Laminar drag reduction in microchannels using ultrahydrophobic surfaces. *Phys Fluids* **16**(12): 4635–4643 (2004)

[280] Kim T J, Hidrovo C. Pressure and partial wetting effects on superhydrophobic friction reduction in microchannel flow. *Phys Fluids* **24**(11): 112003 (2012)

[281] Xia G D, Liu Q M, Qi J Z, Xu J L. Influence of surfactant on friction pressure drop in a manifold microchannel. *Int J Therm Sci* **47**(12): 1658–1664 (2008)

[282] Jian S J, Lin M J. Effect of smooth microchannel cross section shape on friction factor. In: Proceedings of the 2006 1st IEEE International Conference on Nano/Micro Engineered and Molecular Systems, Zhuhai, China, 2006: 1080–1083.

[283] Papautsky I, Gale B K, Mohanty S K, Ameel T A, Frazier A B. Effects of rectangular microchannel aspect ratio on laminar friction constant. In: Proceedings of the Symposium on Micromachining and Microfabrication, Santa Clara, USA, 1999: 147–158.

[284] Sirghi L. Effect of capillary-condensed water on the dynamic friction force at nanoasperity contacts. *Appl Phys Lett* **82**(21): 3755–3757 (2003)

[285] Zamora R R M, Sanchez C M, Freire F L, Prioli R. Influence of capillary condensation of water in nanoscale friction. *Phys Status Solidi A* **201**(5): 850–856 (2004)

[286] Gluzdov D S, Gatapova E Y. Friction reduction by inlet temperature variation in microchannel flow. *Phys Fluids* **33**(6): 062003 (2021)

[287] Tesler A B, Kim P, Kolle S, Howell C, Ahanotu O, Aizenberg J. Extremely durable biofouling-resistant metallic surfaces based on electrodeposited nanoporous tungstite films on steel. *Nat Commun* **6**: 8649 (2015)

[288] Epstein A K, Wong T S, Belisle R A, Boggs E M, Aizenberg J. Liquid-infused structured surfaces with exceptional anti-biofouling performance. *PNAS* **109**(33): 13182–13187 (2012)

[289] Wang D H, Sun Q Q, Hokkanen M J, Zhang C L, Lin F Y, Liu Q, Zhu S P, Zhou T F, Chang Q, He B, et al. Design of robust superhydrophobic surfaces. *Nature* **582**(7810): 55–59 (2020)

[290] Wang N, Zhang R Y, Chan C T. Robust acoustic pulling using chiral surface waves. *Phys Rev Appl* **15**(2): 024034 (2021)

[291] Wu Y, Liu Z L, Liang Y M, Pei X W, Zhou F, Xue Q J. Switching fluid slippage on pH-responsive superhydrophobic surfaces. *Langmuir* **30**(22): 6463–6468 (2014)

[292] Seo J H, Tsutsumi Y, Kobari A, Shimojo M, Hanawa T, Yui N. Modulation of friction dynamics in water by changing the combination of the loop- and graft-type poly(ethylene glycol) surfaces. *Soft Matter* **11**(5): 936–942 (2015)

[293] Schmatko T, Hervet H, Leger L. Friction and slip at simple fluid–solid interfaces: The roles of the molecular shape and the solid–liquid interaction. *Phys Rev Lett* **94**(24): 244501 (2005)

[294] Zhao X J, Kuang S Y, Wang Z L, Zhu G. Highly adaptive solid–liquid interfacing triboelectric nanogenerator for harvesting diverse water wave energy. *ACS Nano* **12**(5): 4280–4285 (2018)

[295] Li X Y, Tao J, Wang X D, Zhu J, Pan C F, Wang Z L. Networks of high performance triboelectric nanogenerators based on liquid–solid interface contact electrification for harvesting low-frequency blue energy. *Adv Energy Mater* **8**(21): 1800705 (2018)

[296] Lin Z H, Cheng G, Lin L, Lee S M, Wang Z L. Water–solid surface contact electrification and its use for harvesting liquid-wave energy. *Angew Chem Int Ed* **52**(48): 12545–12549 (2013)

[297] Wang Y, Gao S W, Xu W H, Wang Z K. Nanogenerators with superwetting surfaces for harvesting water/liquid energy. *Adv Funct Mater* **30**(26): 1908252 (2020)

[298] Wu H, Chen Z F, Xu G Q, Xu J B, Wang Z K, Zi Y L. Fully biodegradable water droplet energy harvester based on leaves of living plants. *ACS Appl Mater Inter* **12**(50): 56060–56067 (2020)

[299] Jeon S B, Seol M L, Kim D, Park S J, Choi Y K. Self-powered ion concentration sensor with triboelectricity from liquid–solid contact electrification. *Adv Electron Mater* **2**(5): 1600006 (2016)

[300] He G, Müser M H, Robbins M O. Adsorbed layers and the origin of static friction. *Science* **284**(5420): 1650–1652 (1999)

[301] Sakuma H, Kawai K, Katayama I, Suehara S. What is the origin of macroscopic friction? *Sci Adv* **4**(12): eaav2268 (2018)

[302] Luo J B. Investigation on the origin of friction and superlubricity. *Chin Sci Bull* **65**(27): 2966–2978 (2020) (in Chinese)

[303] Lin S Q, Xu L, Wang A C, Wang Z L. Quantifying electron-transfer in liquid–solid contact electrification and the formation of electric double-layer. *Nat Commun* **11**(1): 399 (2020)

[304] Sun M Z, Lu Q Y, Wang Z L, Huang B L. Understanding contact electrification at liquid–solid interfaces from surface electronic structure. *Nat Commun* **12**(1): 1752 (2021)

[305] Nie J H, Ren Z W, Xu L, Lin S Q, Zhan F, Chen X Y, Wang Z L. Probing contact-electrification-induced electron and ion transfers at a liquid–solid interface. *Adv Mater* **32**(2): 1905696 (2020)

[306] Leger L, Joanny J F. Liquid spreading. *Rep Prog Phys* **55**(4): 431–486 (1992)

[307] Dussan V E B, Davis S H. On the motion of a fluid–fluid interface along a solid surface. *J Fluid Mech* **65**(1): 71–95 (1974)

[308] Chiricotto M, Giacomelli L. Weak solutions to thin-film equations with contact-line friction. *Interface Free Bound* **19**(2): 243–271 (2017)

[309] Guo S, Gao M, Xiong X M, Wang Y J, Wang X P, Sheng P, Tong P E. Direct measurement of friction of a fluctuating contact line. *Phys Rev Lett* **111**(2): 026101 (2013)

[310] Radha B, Esfandiar A, Wang F C, Rooney A P, Gopinadhan K, Keerthi A, Mishchenko A, Janardanan A, Blake P, Fumagalli L, et al. Molecular transport through capillaries made with atomic-scale precision. *Nature* **538**(7624): 222–225 (2016)

[311] Choi C H, Ulmanella U, Kim J, Ho C M, Kim C J. Effective slip and friction reduction in nanograted superhydrophobic microchannels. *Phys Fluids* **18**(8): 087105 (2006)

[312] Li J C, Zhu Y B, Xia J, Fan J C, Wu H G, Wang F C. Anomalously low friction of confined monolayer water with a quadrilateral structure. *J Chem Phys* **154**(22): 224508 (2021)

[313] Zhang L Y, Wu K L, Chen Z X, Li J, Yu X R, Yang S. Molecular-scale friction at a water–graphene interface and its relationship with slip behavior. *Phys Fluids* **32**(9): 092001 (2020)

[314] Wagemann E, Misra S, Das S, Mitra S K. Quantifying water friction in misaligned graphene channels under ångström confinements. *ACS Appl Mater Inter* **12**(31): 35757–35764 (2020)

[315] Yang L, Guo Y J, Diao D F. Structure and dynamics of water confined in a graphene nanochannel under gigapascal high pressure: Dependence of friction on pressure and confinement. *Phys Chem Chem Phys* **19**(21): 14048–14054 (2017)

[316] Dai H W, Liu S Y, Zhao M Y, Xu Z J, Yang X N. Interfacial friction of ethanol–water mixtures in graphene pores. *Microfluid Nanofluid* **20**(10): 141 (2016)

[317] Tamtögl A, Bahn E, Sacchi M, Zhu J D, Ward D J, Jardine A P, Jenkins S J, Fouquet P, Ellis J, Allison W. Motion of water monomers reveals a kinetic barrier to ice nucleation on graphene. *Nat Commun* **12**(1): 3120 (2021)

[318] Tocci G, Bilichenko M, Joly L, Iannuzzi M. *Ab initio* nanofluidics: Disentangling the role of the energy landscape and of density correlations on liquid/solid friction. *Nanoscale* **12**(20): 10994–11000 (2020)

[319] Keerthi A, Goutham S, You Y, Iamprasertkun P, Dryfe R A W, Geim A K, Radha B. Water friction in nanofluidic channels made from two-dimensional crystals. *Nat Commun* **12**(1): 3092 (2021)

[320] Fumagalli L, Esfandiar A, Fabregas R, Hu S, Ares P, Janardanan A, Yang Q, Radha B, Taniguchi T, Watanabe K, et al. Anomalously low dielectric constant of confined water. *Science* **360**(6395): 1339–1342 (2018)

[321] Luan B Q, Zhou R H. Wettability and friction of water on a MoS_2 nanosheet. *Appl Phys Lett* **108**(13): 131601 (2016)

[322] Lee H, Jeong H, Suh J, Doh W H, Baik J, Shin H J, Ko J H, Wu J Q, Kim Y H, Park J Y. Nanoscale friction on confined water layers intercalated between MoS_2 flakes and silica. *J Phys Chem C* **123**(14): 8827–8835 (2019)

[323] Wang H J, Zhang Z H, Zheng J, Zhao J, Liang Y H, Li X J, Ren L Q. Multifunctional superhydrophobic surface with dynamically controllable micro/nanostructures for droplet manipulation and friction control. *Chem Eng J* **417**: 127944 (2021)

[324] Barthlott W, Schimmel T, Wiersch S, Koch K, Brede M, Barczewski M, Walheim S, Weis A, Kaltenmaier A, Leder A, et al. The salvinia paradox: Superhydrophobic surfaces with hydrophilic pins for air retention under water. *Adv Mater* **22**(21): 2325–2328 (2010)

Zhiran YI. He is a postdoctoral fellow in Department of Mechanical Engineering at City University of Hong Kong, China, and School of Mechanical Engineering at Shanghai Jiao Tong University, China. He received his Ph.D. degree in electronic science and technology from Shanghai Jiao Tong University in 2020. His research mainly focuses on mechanics in smart or soft materials, hydroelectrodynamics, and batteryless biomecial devices.

Xiong WANG. He is a postdoctoral fellow in Department of Mechanical Engineering, City University of Hong Kong, China. He received his Ph.D. degree in Institute of Nuclear and New Energy Technology at Tsinghua University, China, in 2020. His research mainly focuses on droplet and phase transition dynamics under extremely high- and low-temperature conditions.

Kaiqiang WANG. He is a Ph.D. student in Department of Mechanical Engineering at Tsinghua University, China, and a visiting scholar at City University of Hong Kong, China, from 2021 to 2022. He received his B.S. degree from Dalian University of Technology, China, in 2019. His current research mainly focuses on tribology and solid–liquid triboelectric nanogenerator.

Zuankai WANG. He is currently a chair professor in Department of Mechanical Engineering at The Hong Kong Polytechnic University, China. Before that he was a chair professor in Department of Mechanical Engineering at City University of Hong Kong, China. He received his Ph.D. degree in mechanical engineering from Rensselaer Polytechnic Institute, USA, in 2008, his M.S. degree in microelectronics from Shanghai Institute of Microsystem and Information Technology, Chinese Academy of Sciences, China, in 2003, and his B.S. degree in mechanical engineering from Jilin University, China, in 2000. His research mainly focuses on nature-inspired materials and devices.